ELECTRICAL PROPERTIES OF BOROSODASILICATE GLASSES CONTAINING Sb$_2$ O$_3$ AND Bi$_2$ O$_3$

A Thesis Submitted
in Partial Fulfilment of the Requirements
for the Degree of
MASTER OF TECHNOLOGY

By
B. V. HIREMATH

to the

INTERDISCIPLINARY PROGRAMME IN MATERIALS SCIENCE
INDIAN INSTITUTE OF TECHNOLOGY KANPUR
AUGUST, 1976

(ii)

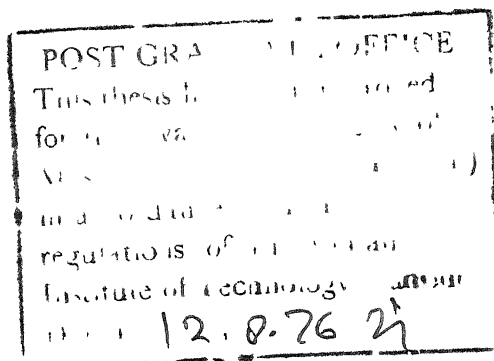# CERTIFICATE

This is to certify that this work on "Electrical Properties of Borosodasilicate Glasses Containing Sb_2O_3 and Bi_2O_3" by B.V. Hiremath has been carried out under my supervision and has not been submitted elsewhere for a degree.

(D. Chakravorty)
Professor
Department of Metallurgical Engineering
Indian Institute of Technology, Kanpur

MS-1976-M-HIR-ELE

ACKNOWLEDGEMENT

I express my heart felt gratitude to Professor D. Chakravorty for his excellent and enthusiastic guidance throughout the course of my research work.

I am thankful to Prof. E.C. Subbarao for his advice and encouragement.

My sincere thanks are due to Mr. Devendra Kumar, Mr. Halliyal Arvind and Mr. H.R. Aravinda for their help in experimental work.

The help rendered by Mr B. Sharma, Mr. R.D. Prasad and Mr. O.P. Malaviya is gratefully acknowledged.

My thanks are also due to Mr. R.N. Srivastava for his excellent typing and Mr. Vishwanath Singh for his help.

B.V. Hiremath

CONTENTS

LIST OF FIGURES

SYNOPSIS

An investigation of electrical, switching and optical properties of various glasses containing both Sb_2O_3 and Bi_2O_3 in Na_2O-B_2O_3-SiO_2 glass matrix was carried out.

The variations of bulk conductivity of these glasses and surface conductivity of virgin glasses, $Na^+ \rightleftharpoons Ag^+$ ion-exchanged and reduced and simply reduced glasses in hydrogen were studied as a function of temperature.

The rigidity of the borosodasilicate glass matrix is found to depend on the ratio of concentration of Sb_2O_3 to Bi_2O_3. The d.c. conductivity in the bulk glasses in the temperature range 50-400°C is believed to arise from movement of alkali ions. The surface resistivities of virgin glasses are higher than those of ion-exchanged and reduced or simply reduced glasses. Ionic conduction and electronic conduction are believed to be effective in determining the surface conductivities. At low temperatures the electronic hopping between two conducting islands is believed to give low activation energy for ion-exchanged and reduced glasses.

Some of ion-exchanged and reduced glasses were found to exhibit "memory" type of switching.

CHAPTER 1

INTRODUCTION

In recent years there has been a tremendous revival
of research activities in amorphous materials mainly due to
the projected technological importance of these materials.
Because of ease of fabrication of amorphous switches in
planar or sandwiched structure and the possibility of direct
incorporation into integrated circuits, these materials are
considered to have tremendous application potential[1].
The wide spectrum of applications of these materials includes
switching and memory devices, continuous dynode electron
multipliers, optical mass memories, high energy particle
detectors, phase contrast holograms, infrared lenses,
ultrasonic delay lines and microfiche transparencies.

1.1 Classification of Amorphous Semiconductors

The examples for various kinds of amorphous semi-
conductors are, elemental such as S and Se[2] and compounds
like vanadate-phosphate[3,4], vanadate-germanate[5],
Ge-Te[6], $As_2Te.Tl_2Se_3$[7], As_2Te_3[8], $4As_2Se_3.2Sb_2Se_3$[9],
As_2S_3[10], $V_2O_5-GeO_2-BaO$[11], $TiO_2-B_2O_3-BaO$[12] etc.

These glasses can be broadly classified according
to their structural and chemical composition, into 3 categories
viz., (1) elemental, (2) covalent alloys and (3) ionic or
tightly bound.

The first category contains elements, of which
only S and Se can be obtained in amorphous form by slow
cooling of their melts. Because of their chain or ring
structure, the short range order extends over rather long
distances depending on temperature and thermal history of
the material. The second category contains alloys of
group IV, V and VI. These possess compositional as well as
translational disorder. The materials belonging to the
third category have positional disorder and impurities as
an additional type of disorder. These materials have band
gaps larger than 2 eV.

1.2   Characteristics of Amorphous Semiconductors

Several phenomena in amorphous semiconductors can
be observed with sufficient frequency to regard them as
characteristic of amorphous phase and they are:

1.   Electrical or thermal energy gaps of approximately
     the same magnitude as those occurring in the
     crystalline phase (where this exists)[13-15].

2. Coexistance of two basic conduction mechanisms, band conduction and hopping between localized states[16].

3. Conductivities which increase with frequency of the applied field[17].

4. Non-ohmic behaviour at high fields[18,19] (followed by switching in some materials).

5. Temperature activated drift mobilities[20,21].

6. Anomalous Hall effect[22].

7. Electrical field dependent quantum efficiency[23,2].

8. Exponential optical absorption edges[23].

9. Optical energy gap greater than electronic energy gap[24,25].

10. Relaxation of the k-conservation selection rule for optical transitions[26].

1.3 Electrical Conductivity

Conduction in glasses can be either ionic or electronic in nature depending upon the nature of glass and the temperature range.

1.3.1 Ionic conductivity

The basic ingredients of oxide glasses are a "network former" e.g., SiO_2, "modifier" e.g., Na_2O, CaO

and an "intermediate" e.g., Al_2O_3. These modifiers are
electrostatically attached to the "non-bridging" oxygen ions
and they are considered to be the principal carriers.

Oxide glasses containing large amounts of alkali
ions are essentially electrolytic conductors as shown by
Littleton et al.[27]. The ionic conductivity of many oxide
glasses results from the transport of monovalent cations,
and usually the mobility of divalent ions is low relative
to alkali ions.

1.3.2 Temperature dependence of ionic conductivity

The electrical resistivity ζ of most of the oxide
glasses is generally described by Rasch-Hinrichsen[28]
relation

$$\log \zeta = A + B/T \tag{1.1}$$

where A and B are constants.

The theoretical model used by Frenkel[29] for
ionic transport in crystalline solids is generally adopted
for glasses, in which an alkali ion will move from one
potential well to another, preferentially in the direction
of applied field.

Various models to explain the relationship
between conductivity, temperature and the nature of the

glass network have been proposed by Stevels[30] and Mazurin[31].

1.3.3 Ionic conductivity and ionic diffusion

From the theoretical considerations on the random jump of ions as the rudimentary step leading to ionic behaviour, it is obvious that ionic conductivity is closely related to ionic diffusion[32]. The electrical conductivity of glass is related to the diffusion coefficient of the ion by Nernst-Einstein relation[33]

$$\sigma = \frac{Z^2 F^2 D C}{RT} \qquad (1.2)$$

where D is the ionic diffusion coefficient in cm^2/sec, F is the Faraday constant, R is the gas constant in Joules/mole-deg., C is the concentration of ions in $moles/cm^3$ and Z is the ionic valence. Equation (1.2) is useful in assessing conduction mechanisms in glasses and it has been found that calculated data are in confirmation with the experimental data[32,33].

1.3.4 The mixed alkali effect

When a second alkali is added to an alkali silicate glass the conductivity decreases sharply[34]. The

mixed alkali effect has been reported for a wide variety of oxide glasses besides silicate glasses like borates, germanates etc. However, for any significant effect, the alkali concentration should exceed 10%[35]. Many theoretical models have been proposed to explain the mixed alkali effect.

It has been also found that ionic conductivity of oxide glasses depends on the composition of the glass[36], applied pressure[37] and thermal history of the glasses[38].

1.4 Electronic Conduction

In most of the amorphous semiconductors conduction is considered to take place by hopping of carriers from one strongly localised state to another. For example, glasses containing transition element such as Fe in $V_2O_5-P_2O_5$, hopping of carriers will take place from one valence (local-ised) state to another of transition metal. The conductivities of these glasses vary according to the relation $\sigma = \sigma_0 \exp(- E/kT)$ where σ_0 is constant and E is activation energy.

1.4.1 Theory of amorphous semiconductors

Several theories have been proposed to explain the electronic conduction in these materials which will be discussed in the next section.

Most of the theoretical approaches have started with standard band theory of crystalline solids and have assumed perturbations to this model, the perturbation taking the form of annihilating the long range order, over a few atomic spacings whilst maintaining the short range order.

In Cohen-Fritsche-Ovshinky[39] model, each localised imperfection is considered to be a 'localised' state in the gap between two bands, due to variation in potential energy. A carrier in the localised states moves by Phonon-assisted hopping and its mobility is therefore less by 2 or 3 orders to that of in "extended" states where the carriers are subjected to many scattering process, Hence there exists a "mobility gap" which replaces the density states gap in case of crystalline semiconductors.

Mott[40-42] has used theory of Anderson[43] to account for the existence of localised states. He has shown that there is a discontinuous change in conductivity at the band edges. Gubanov[44] considered the glassy model as a "frozen" liquid in which potential wells of random depth are assumed to give rise to localised states.

It is to be noted that all the models predict "tail" states extending to several tenths of an eV and localised states densities of 10^{18}-10^{19} cm^{-3}. We notice that these models differ in their origin for the cause of

the localised states. Cohen finds they arise from density fluctuations in a random atomic structure; Mott—from random well depths in a periodic well structure; and Gubanov — from random spacings of wells of uniform depth with a small effect due to well depth variations. All these models have been recently reviewed by Hulls et al.[45].

1.5 Switching Properties

One of the most interesting properties of glasses is the phenomenon of electronic switching. There are two types of switching[46]; threshold switching and memory switching.

1.5.1 Threshold switching

As the applied voltage of the sample is increased, at a critical voltage called "threshold" voltage, the material switches from high resistance ("OFF") state to low resistance ("ON") state and below a certain holding current through it, the material switches back to OFF state. This is reversible. The threshold voltage is found to depend on temperature as well as separation between the electrodes.

Many mechanisms have been put forward to describe the threshold switching and they are:

(i)   Electronic mechanism[47,48]

(ii)   Phase change mechanism[49,50]

(iii) Purely thermal breakdown[51,52].

However, no theory is complete in accounting for all the switching of the glasses.

1.5.2 Memory switching

As we increase the voltage across the material it switches to "ON" state. The conductive "ON" state will be maintained even after the switching voltage is removed. In other words an irreversible transformation from an insulating state to a conductive state has occurred. Through proper pulsing the material can be made to return to "OFF" state. The memory effect has generally been associated with a glass-to-crystal transition. Conductivity could be due to the formation of filaments embedded in the glass and bridging the electrodes. While pulsing the remelting of the filaments occurs which results in high conductive "OFF" state.

Whether a glass will show "threshold" or "memory" behaviour is dependent on its chemical composition. For instance, a glass with composition 10Ge - 30As - 12.6Si - 47.7Te (atomic %) shows threshold switching whereas another

one with composition 10Ge - 50As - 40Te (atomic %) shows memory behaviour[52].

1.6 Ion-Exchange and Reduction Treatments

1.6.1 Reduction

It is found that resistivities of certain oxide glasses will decrease if the surface is given reduction treatment by hydrogen. Green and Blodgett[53] have studied the electrical properties of Bi_2O_3 and PbO glasses after subjecting to reduction treatment by hydrogen. They have found that the surface conductivity of the reduced glasses was as low as 100-1000 ohm/square. The surface conductivities of the reduced glasses were found to depend on the distance between the particles, influence of surrounding oxide lattices and composition of the glasses[54].

1.6.2 Ion-exchange and reduction

When a glass is immersed in molten bath like $AgNO_3$, or CuCl or $CuCl_2$, at the glass-salt interface ions move in and out of the glass governed by ion-exchange mechanism. If the ion-exchange treatment is carried out above the glass transition temperature T_g, the network of glass adjusts itself to the differing partial molar volumes

of the exchange ions. When the temperature is less than T_g it results in a stress in the glass. If the salt bath ions are larger than the host ions in the glass there is a resultant /compression which increases the strength of the glass[55].

1.7   Studies of Glasses Containing Antimony Oxide and Bismuth Oxide

Several glasses containing $B_2O_3-Bi_2O_3$, $B_2O_3-Sb_2O_3$, $CaO-Bi_2O_3$, $Al_2O_3-Bi_2O_3$. $PbO-B_2O_3$ in Na_2O-SiO_2 base glass matrix and "float" glass containing $SiO_2-Na_2O-CaO-MgO-K_2O-SO_3-Al_2O_3-Fe_2O_3$ have been extensively studied by Chakravorty et.al.[56,57] The former group glasses was treated with sodium - silver ion exchange followed by reduction in hydrogen whereas the latter group was treated with sodium ⇌ copper ion exchange and ion reduction in hydrogen.

1.7.1   Microstructural studies

It has been found that the microstructural features of all the glasses containing Bi_2O_3 were similar. The electron micrographs of the surface of the virgin glass reveals that it consists of a dispersion of spherical particles of metallic bismuth with diameters ranging from 50-800 Å, embedded in glassy matrix. After ion exchange and subsequent reduction larger particles with maximum

diameter of about 2000 $\overset{\circ}{A}$ metallic silver are found to appear in the glass matrix.

However, the droplet phase in virgin specimen of Sb_2O_3 containing glass is found to be rich in antimony but not in metallic state. The ion exchanged and reduced specimen has a structure consisting of fine silver droplets of diameters measuring from 50-100 $\overset{\circ}{A}$.

In case of Al_2O_3 containing glasses the droplet phase in virgin sample is rich in bismuth which however is not in metallic state. After ion exchange and reduction the droplets become much smaller ranging from 50-150 $\overset{\circ}{A}$ and after reduction metallic silver droplets appear having diameters measuring from 50-650 $\overset{\circ}{A}$.

It is to be noted that in all the cases metallic silver particles with diameters measuring from 50-2000 $\overset{\circ}{A}$ are found to appear in dispersed glass matrix.

The electron micrograph of the surface of "float"[57] glass shows no phase separation before ion exchange and reduction treatment. After (copper-sodium) ion exchange done at high temperature (650°C) the sample shows phase separation due to injection of copper ions into glass.

1.7.2 Switching studies

Memory switching has been observed by Chakravorty[58] and Devendra Kumar[59] in surface layers containing Bi_2O_3 and Sb_2O_3 separately in $Na_2O-B_2O_3-SiO_2$ base glass matrix. Chakravorty and Murthy[60] have observed negative resistance and memory switching in thin films of $Na_2O-Bi_2O_3-B_2O_3-SiO_2$ glasses.

The switching observed in bismuth glasses has been ascribed to its microstructural characteristics. The sample switches to the "ON" state upon application of an electric field which presumably induces crystallisation of the glass phase between the metallic bismuth "islands". A high current pulse of short duration melts these crystals which are then quenched back to the glassy phase to give "OFF" state.

It is to be noted that the surface roughness of the glasses is necessary for obtaining the high conductance effect. It is believed that imperfections introduced in the surface by grinding operation increase the efficiency of metallic particles which can then grow sufficiently to form a continuous chain.

Chakravorty et.al.[60] have attributed the possibility for the "OFF" state conduction to the electron

hopping between conducting islands of bismuth in case of thin films of bismuth glasses. The activation energy for electron hopping in such a situation has been shown by Neugebauer and Webb[64] to be given by e^2/Kr where e is the electronic charge, K is the dielectric constant of the glassy matrix, and r is the diameter of the conducting island. Assuming a value of K = 6 (Chakravorty et.al.[61]) one calculates from the spread of activation energies mentioned above a range of r values extending from 10-150 $\overset{o}{A}$. This is consistent with the microstructural features of these glasses as we have seen in earlier section.

The negative resistance obtained in these glass films is considered to arise from a Joule-microheating process[62]. It has been found by extrapolation of the plot of threshold voltage versus temperature for the glass films, that at about 450°C, the glass film would switch without application of electric field and switch off temperature was found close to melting point of bismuth metal. These glasses tend to crystallize in the temperature range 500-600°C, the crystalline phase having a lower resistance than the parent glass[61].

Thus they conclude that if the "ON" state is assumed to be a result of the formation of bismuth filaments between conducting islands, the switch "OFF" process can

be explained on the basis of a rupture of the filaments.

1.7.3 Anomalous behaviour of Sb_2O_3 and As_2O_3 glasses

Oxide glasses containing Sb_2O_3 in $Na_2O-B_2O_3-SiO_2$ glass matrix have shown very interesting properties. The resistivities of the ion exchanged and reduced surface of the glasses have been shown by Devendra Kumar[59] to have a marked dip at around room temperature.

Similar behaviour has been found by Halliyal Arvind[63] in glasses containing As_2O_3 in $Na_2O-B_2O_3-SiO_2$ glass matrix. He has observed that the surface resistivities of all the virgin, reduced and ion exchanged and reduced glasses exhibit a minimum near room temperature. The resistivities increase both below room temperature and just above room temperature. The increase in resistivity below room temperature is tentatively attributed to proton conduction and the increase just above room temperature is described as due to water molecules and their interaction with silicate network of the glass.

Since alkali borosilicate glasses containing Sb_2O_3 and Bi_2O_3 respectively have shown memory switching behaviour after ion exchange and reduction, it was thought that it would be interesting to study the conduction mechanisms and switching properties, when both Bi_2O_3 and Sb_2O_3 are incorporated in the same $Na_2O-B_2O_3-SiO_2$ glass matrix.

CHAPTER 2

STATEMENT OF THE PROBLEM

Electrical properties of glasses containing Sb_2O_3 and Bi_2O_3 separately in $Na_2O-B_2O_3-SiO_2$ glass matrix have been studied earlier, and it has been found that these glasses show memory type of switching after ($Na^+ \rightleftharpoons Ag^+$) ion-exchange and reduction treatment. It was thought it would be interesting to study the conduction mechanisms and switching properties when both Bi_2O_3 and Sb_2O_3 incorporated in the same $Na_2O-B_2O_3-SiO_2$ glass matrix.

The objectives of the present investigation were to study the following:

(a) Bulk properties: Variation of bulk resistivity of glasses with temperature.

(b) Surface properties: Variation of surface resistivities of virgin, reduced and ion-exchanged and reduced glasses with temperature.

(c) Switching properties: To study the switching properties of ion-exchanged and reduced glasses at room temperature and below room temperature.

(d) Optical properties: To study the absorption spectra of virgin glasses in the visible range.

(e) Differential thermal analysis.

(f) To study the above effects as a function of the ratio of concentration of Sb_2O_3 to Bi_2O_3 present in the borosilicate glass system.

CHAPTER 3

EXPERIMENTAL PROCEDURE

3.1 Glass Preparation

The glasses containing varying amounts of Sb_2O_3 and Bi_2O_3 were prepared from reagent grade chemicals. The compositions are listed in Table 1. Na_2O was introduced as carbonate, B_2O_3 as boric acid and rest of the ingredients as oxides. The calculated amounts of the starting materials were mixed with acetone and dried. The dried mixture was taken in a high density alumina crucible and heated electrically in a furnace fitted with globar rods. Temperatures of melting of these glasses were in the range of 1300-1450°C. The melt was poured without keeping for a long time in the molten state into aluminium molds of dimensions about 5 cm x 1 cm x 0.5 cm. Since it was observed that Bi_2O_3 oozes out through the tiny pores of the crucible at high temperature the batch was not kept in molten state for a long time. The glasses were annealed at about 400°C and were furnace cooled over night.

The glasses containing less mole % of Na_2O like glasses 11-23 were difficult to melt and hence it was necessary to keep the melt at high temperature for a longer time for homogenization.

3.2   Sample Preparation

3.2.1   Bulk resistivity measurements

The glass plates of dimensions approximately
2 cm x 1 cm x 1 cm were polished to a thickness of 0.5-1 mm
using silicon carbide grit of different mesh sizes (120, 240.
400, 600 and 800 respectively). The silver electrodes were
painted uniformly using silver paste (supplied by NPL,
India) on both the surfaces and copper wires were affixed
to the electrodes. After the paint dried, the specimens
were sandwiched between two glass plates (microscope
slides) for mechanical support. A guard ring configuration
was used to measure the bulk resistivities of the samples.

3.2.2   Surface resistivity measurements

Glass pieces of dimensions approximately 2.0 cm x
1 cm x 0.25 cm were polished using silicon carbide mesh
no. 120 for surface resistivity measurements.

For ion-exchange and reduction, these polished
glasses were immersed in molten $AgNO_3$ bath kept in pyrex
crucibles which were heated at 320°C for 6 hours. They
were washed in running water to remove any silver nitrate
adhering to the surfaces of glasses and then they were
given reduction treatment in hydrogen as follows.

The ion-exchanged samples were kept in a furnace and hydrogen gas was passed at a rate of 100 c.c. per minute and the temperature was raised slowly to 320°C. The reduction treatment was carried out for 12 hours. Then these were furnace cooled. Parallel silver electrodes were painted on the surface and copper wires affixed to them as described above. A schematic diagram of the electrode configuration is shown in Fig. 11. Araldite was put on copper leads for mechanical support.

Only reduction treatment was given after polishing another set of samples and electrode leads were fixed as described earlier.

To the virgin glass samples also the electrode leads were put after polishing the sample.

3.3 Resistivity Measurements

Bulk resistivity and virgin glass surface resistivity for all the glasses were measured from room temperature to about 400°C, whereas the reduced and ion-exchanged and reduced surface resistivities were measured from room temperature to 320°C, since ion-exchange and reduction treatments were carried out at 320°C. This was to avoid any effect of heat treatment given to the sample by going beyond the temperature at which ion-exchange and reduction treatments were carried out.

3.3.1 High temperature resistivity measurements

The circuit used to measure resistivities is as
shown in Fig. 1. The sample was put in a horizontal furnace
fitted with Aplab temperature controller. The sample was
surrounded by metallic tube and the tube was earthed for
better shielding purpose. The temperature was increased in
steps of 15-25°C and at each constant temperature. (the
temperature could be kept constant to within ± 2°C) the
V-I characteristics of the samples were measured either
using voltage measuring device like G.R. Electrometer (type
1230-A) or current measuring device like ECIL Digital
Picoammeter (type EA813A).

3.3.2 Low temperature resistivity measurement

For low temperature resistivity measurement, a
set-up given in reference[59] was used. The same circuit
as used in the high temperature was used to obtain the V-I
characteristics. ECIL Electrometer (type EA814) was used
as the voltage measuring device.

The V-I characteristics were then fitted to
straight line by a least square method using a computer
program. The resistivities were calculated by computing
slope of these lines.

3.4 Switching Properties

Switching characteristics of ion-exchanged and reduced samples were obtained using the same circuit as in the case of high temperature resistivity measurements. For "ON" state characteristic a high resistance (10^5 ohms) was connected in series to sample, to control the current through the circuit.

3.5 Optical Absorption Spectra

The virgin glass samples were polished to a thickness of about 0.5 mm using silicon carbide grit of different mesh sizes. Absorption spectra of these samples were recorded using Cary-14 spectrometer in wavelength range 2000-6000 $\overset{o}{A}$. Since ion-exchanged and reduced samples were black, the absorption spectra for these samples could not be obtained.

3.6 Differential Thermal Analysis

DTA was carried out taking fine powdered samples of few glasses using "Mom Derivetograph" in the temperature range room temperature to 1000°C by increasing the temperature at a rate of 10°C/min. Pt-Pt/Rh thermocouple and Al_2O_3 reference material were used in the investigation.

CHAPTER 4

RESULTS

The variation of resistivity with temperature is
described by the equation

$$\rho = \rho_O \ \exp(E/kT) \tag{4.1}$$

where E is activation energy, ρ_O is a constant and k is
Boltzmann constant. If to the first approximation plots of
log ρ vs 1/T are straight lines, the activation energy E
and the constant ρ_O in the equation (4.1) can be calculated
using the standard least squares method of fitting the data.

4.1 Bulk Resistivity Measurements

The variation of bulk resistivities of different
glasses in the temperature range 30-400°C are given in
figures '2 to 9.. The activation energy calculated in
different regions of the plots are given in Table 2.

The bulk resistivities of glasses 1, 2, 3, 4, and
5 show similar variation of resistivity with temperature.
In the temperature range 20-150°C, the activation energies
vary from 0.3 eV to 0.9 eV. In the temperature range
200-310°C activation energies vary from 0.1 to 0.5 eV.

In most of the glasses cooling cycle curves become linear
and they differ from heating cycle curves. The bulk resis-
tivities of glasses 12, 21 and 23 are higher than that of
glasses 1, 2, 3, 4 and 5. In the case of glass 3, during
cooling from 400°C, it switched from a high resistance
state (10^7 ohm-cm) to low resistance state (10^5 ohm-cm).
This low resistance/state was quenched using liquid nitrogen, "ON"
state characteristics were obtained.

The variation of activation energy calculated in
temperature ranges 20-150°C and 200-310°C, with ratio of
concentration of Sb_2O_3 to Bi_2O_3 is shown in Fig. 10. We
observe that in the former temperature range the activation
energy shows a maximum value when the ratio Sb_2O_3/Bi_2O_3 is
about one. Whereas in the latter temperature range the
activation energy decreases when the ratio Sb_2O_3/Bi_2O_3
increases.

4.2 Surface Resistivity Measurements

4.2.1 Virgin glasses

The surface resistivities of virgin glasses with
no surface treatments (ion-exchange or reduction) were
measured from room temperature to 400°C. The surface
resistivity in ohm/square was calculated using the relation

$$\rho = \frac{RA}{B}$$

where R is the resistance of the sample in ohms, A is width of electrode and B is the gap of electrode. Geometry of electrodes is shown in Fig. 11.

The variation of log ζ (ohm/□) with inverse of absolute temperature for virgin glasses 1, 3, 4 and 5 is linear as shown in Fig. 11. For all the glasses the surface resistivities during heating cycle and cooling cycle are approximately the same. Activation energies for the glasses are of the order of 1.0 eV. Virgin glasses 11, 12 and 13 show a hump in log ζ (ohm/□) vs. 1/T plot at about 120°C as shown in Fig. 12. The values of surface resistivities for all these glasses are of the order of 10^{14} ohm/□ . The energies for the glasses above 120°C are of the order of 1.0 eV whereas for temperatures below 120°C, they are of the order of 0.5 eV. It is to be noted that, for the temperatures above 120°C the activation energies for all the glasses are of the same order irrespective of the ratio of concentration of Sb_2O_3 to Bi_2O_3. The cooling cycle curve show similar behaviour but the orders of magnitude of the resistivities during cooling cycle are smaller than heating cycle.

4.2.2 Reduced glasses

Some of the glasses were only reduced in a current
of hydrogen gas without ion-exchange treatment for 12 hours
at 320°C. The surface of the reduced glasses were measured
in the temperature range 30° to 320°C. Activation energies
of different regions of the plot of log $\int$ vs. 1/T are
tabulated in Table 2.

The variation of resistivity with temperature of
reduced glasses 2 and 3 are shown in Fig. 13. It is
observed that the plots are linear in the above temperature
range. In case of glass 2, cooling cycle curve agrees with
heating cycle curve. For glass 3, even though the cooling
cycle values of resistivity are slightly higher than that
of heating cycle, the variation is similar in both the
cycles. Glasses 11 and 12 also show linear behaviour in
the temperature range 30-250°C and activation energies are
of the order of 0.2 eV. The cooling curves for the glasses
differ slightly from heating curves. The plots of log ρ
vs. 1/T of glass 13 is shown in Fig. 15. Between 50 to 150°C
the surface resistivity of the glass was too high to be
measured. Cooling curve also shows similar behaviour
even though the resistivities of cooling cycle are lower
than that of heating cycle. However, it is to be noted

that the orders of magnitude of resistivity are lower than
that of virgin glasses.

4.2.3 Ion-exchanged and reduced (IER) glasses

All glasses were given first ($Na^+ \rightleftharpoons Ag^+$) ion-
exchange treatment at 320°C for 6 hours in molten $AgNO_3$ bath
and then reduced in hydrogen atmosphere at 320°C for 12
hours. The surface resistivities were calculated from
measured resistances of the samples at different temperatures,
as described earlier. The resistances of the sample were
measured in the temperature range -100 to 320°C. The plots
of log τ (ohm/$\Box$) vs 1/T are shown in figures 16 to 23.
In the case of IER glasses 3, 4, 5 and 21 minima are
observed in the plots of log $\jmath$ vs 1/T. It is seen that as
the ratio of the concentration of Sb_2O_3 to Bi_2O_3 increases,
(from 1 to 5) the minima move (from room temperature to
70°C) towards high temperature.

IER glasses 1 and 2 show two activation energies
in the temperature range of about -90° to 320°C. IER
glasses 12, 22 and 13 show linear behaviour in the temper-
ature range 20°C to 320°C. The activation   energies of
the glasses are 0.17, 0.18 and 0.34 respectively. For
IER glasses also, the orders of magnitude of surface
resistivities are less than that of virgin glasses.

4.3 Switching Studies

I-V characteristics of some IER glasses are shown in figure: 24 . at room temperature. IER glass 1 switches from high resistance state (2.2×10^8 ohm) to low resistance state (1.9×10^6 ohm) at voltage of 250 V. IER glass 4 switches from 4.5×10^8 ohm to 4×10^6 ohm at 200 V. For IER glass 2 the switching voltage is very low (5.7 volts). The "OFF" state resistance is of the order of 6×10^8 ohm and "ON" state resistance is of the order of 8×10^3 ohm. There is high instability near switching voltage. After few cycles the "ON" state got stabilised for the glass. Switching characters were also obtained at low temperatures. There was no regular variation of threshold switching voltage/with temperature.

4.4 Optical Absorption

Optical absorption spectra for few virgin glasses were recorded using Cary-14 spectrometer in the wavelength range of 2500-6500 $\overset{o}{A}$. The absorption coefficients were calculated at different wavelengths from the optical spectra using the relation

$$\alpha \;=\; \ln \frac{I_o}{I} \frac{1}{x} \; cm^{-1} \qquad\qquad (4.1)$$

where I is the transmitted intensity and x is the thickness of the sample. A plot of $(\alpha h\nu)^{\frac{1}{2}}$ vs. $h\nu$ gives the optical absorption edge E_{opt}, by extrapolating the linear part of the plot as described by Tauc et.al.[66]

From the absorption spectra recorded for the glasses, plots of $(\alpha h\nu)^{\frac{1}{2}}$ vs. $h\nu$ were made. Optical gaps thus obtained lie in the range of 2.7 to 3.6 eV, as shown in Fig. 25.

4.5 Differential Thermal Analysis

DTA curves for glass 2 and 3 are shown in Fig.26. For glass 2 three minima were observed at about 80, 560 and 800°C respectively. A peak was observed at 780°C. For glass 3 a broad dip was observed at 580°C and a small peak at 790°C.

Table 1

The chemical composition of the glasses

Glass No.	Composition in mole %					
	Na_2O	B_2O_3	Bi_2O_3	Sb_2O_3	SiO_2	K_2O
1	10	18	10	2	60	–
2	10	15	10	5	60	–
3	10	16	5	5	64	–
4	10	15	5	10	60	–
5	10	18	2	10	60	–
11	5	21	5	5	64	–
12	3	22	5	5	64	1
13	1	23	5	5	64	2
21	5	20	5	10	60	–
22	3	21	5	10	60	1
23	1	22	5	10	60	2

Table 2

Activation energy E calculated from log γ vs. 1/T plots for different regions of the curves for glasses studied, as computed using method of least squares

Glass No.	Fig. No.	Inverse temperature range (1/T)		Region marked on the graph	Activation energy eV	Standard deviation eV
		From	To			
I Bulk resistivity						
1	2	1.7	2.0	(a)	0.47	0.10
		2.4	3.4	(b)	0.53	0.04
		1.6	2.6	(c)	1.10	0.02
2	3	1.7	2.4	(a)	0.26	0.02
		2.5	3.4	(b)	0.91	0.04
3	4	1.5	2.9	(a)	0.31	0.01
		3.9	5.4	(b)	0.23	0.01
4	5	1.7	2.4	(a)	0.28	0.02
		2.5	3.4	(b)	0.79	0.05
5	6	1.7	2.1	(a)	0.13	0.03
		2.4	3.4	(b)	0.67	0.04
		1.7	2.7	(c)	1.08	0.03
12	7	1.5	2.1	(a)	0.55	0.01
21	8	1.4	1.8	(a)	1.42	0.09
		2.0	2.5	(b)	1.11	0.11
23	9	1.4	2.2	(a)	0.77	0.06
		2.2	3.0	(b)	0.40	0.02

Table 2 (Continued)

Glass No.	Fig. No.	Inverse temperature range (1/T)		Region marked on the graph	Activation energy eV	Standard deviation eV
		From	To			
		II	Surface resistivity			
		A.	Virgin glasses			
1	11	1.4	2.4	(a)	1.07	0.03
3	11	1.4	2.4	(a)	1.03	0.08
4	11	1.4	2.6	(a)	1.07	0.02
5	11	1.4	2.6	(a)	0.96	0.03
11	12	1.5	2.5	(a)	-0.81	0.03
		2.5	3.2	(b)	-0.51	
12	12	1.4	2.0	(a)	1.04	0.02
		2.5	3.2	(b)	0.50	
13	12	1.4	2.0	(a)	1.05	
		2.5	3.2	(b)	0.50	
		B.	Reduced glasses			
2	13	1.8	3.2	(b)	0.21	0.01
3	13	1.7	2.3	(a)	0.55	0.03
		2.3	3.2	(b)	0.28	0.02
		1.7	2.7	(c)	0.54	0.02
11	14	1.7	3.1	(b)	0.22	0.05
12	14	1.7	3.1	(b)	0.19	0.01
13	15	1.7	2.2	(a)	0.73	0.07
		2.1	2.8	(b)	0.47	0.20

Table 2 (Continued)

Glass No.	Fig. No.	Inverse temperature range (1/T)		Region marked on the graph	Activation energy eV	Standard deviation eV
		From	To			
		C.	Ion-exchanged and reduced glasses			
1	16	1.8	3.0	(a)	0.66	0.02
		3.0	5.5	(b)	0.08	0.03
2	17	2.0	3.0	(a)	0.15	0.02
		3.5	5.0	(b)	0.08	0.004
3	18	2.0	2.6	(a)	0.69	0.04
		2.7	3.2	(b)	0.87	0.25
4	19	3.2	4.6	(b)	0.13	0.01
5	20	1.9	2.5	(a)	0.64	0.02
		3.3	3.8	(b)	0.77	0.09
11	21	2.4	3.3	(b)	0.58	0.04
		2.2	3.1	(a)	0.77	0.01
12	22	1.8	3.2	(b)	0.17	0.01
13	22	1.8	3.2	(b)	0.34	0.07
21	23	1.8	3.0	(b)	0.57	0.03
22	22	1.7	3.2	(b)	0.19	0.01

Digital picoammeter/E.meter

0.5mm

D.C.Power
supply

(a)

Digital pico-
ammeter/E.met-
er

D.C.Power
supply

(b)

FIG.1   SCHEMATIC CIRCUIT DIAGRAM FOR

(a) Bulk resistivity measurement
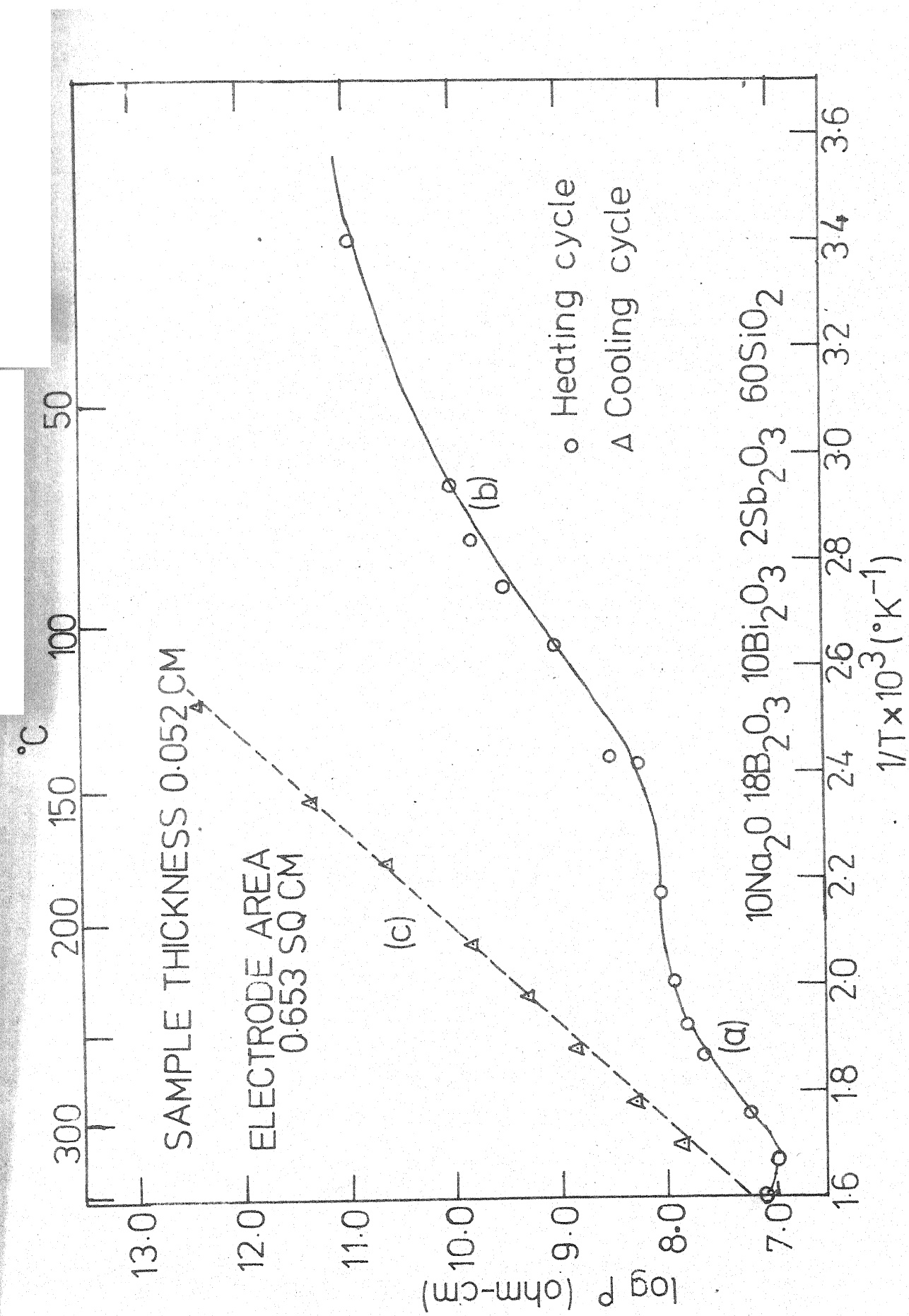(b) Surface resistivity measurement

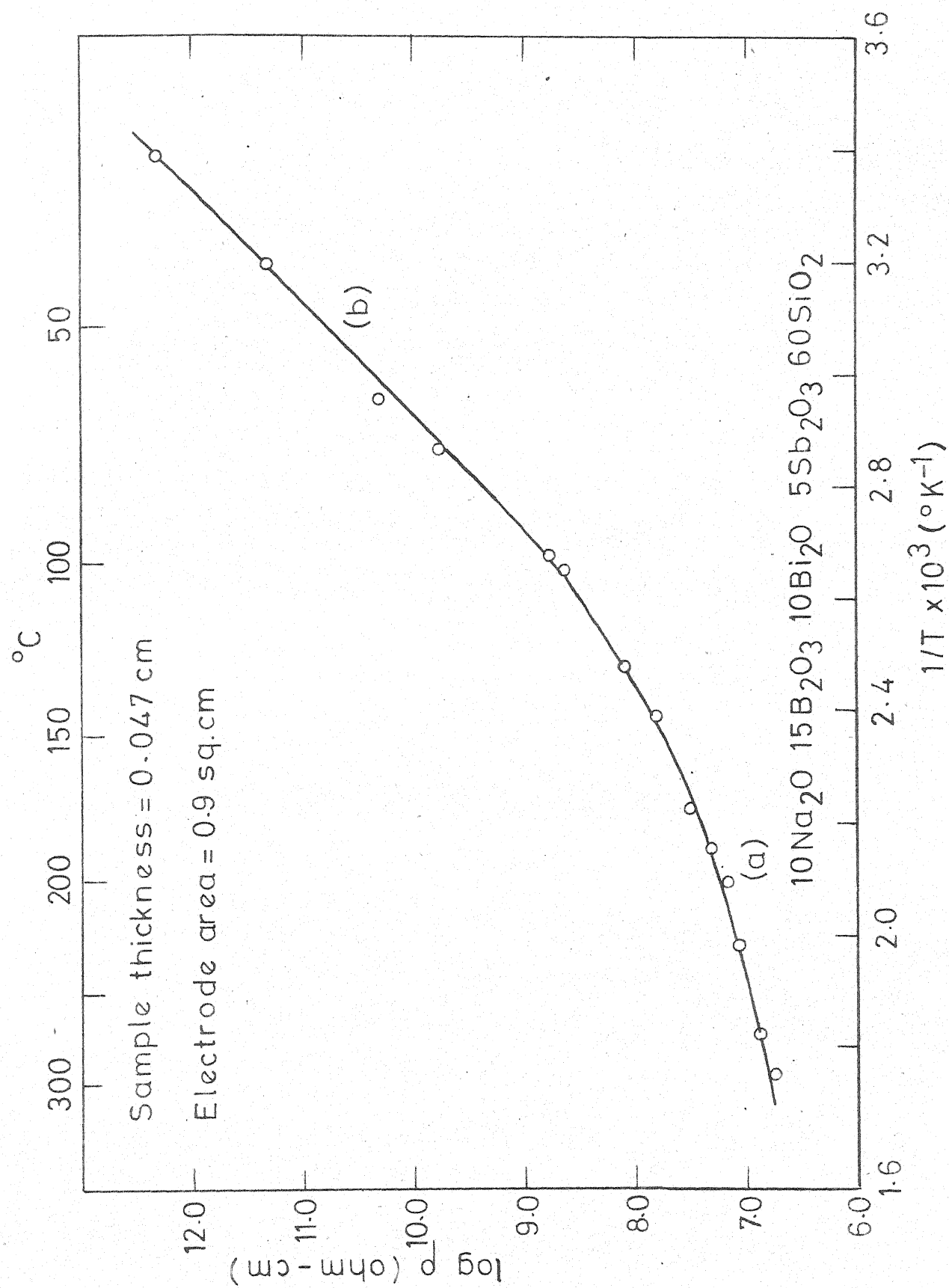FIG.2 VARIATION OF BULK RESISTIVITY WITH TEMPERATURE FOR GLASS NO.1

Fig. 3 Variation of bulk resistivity with temperature for glass 2.
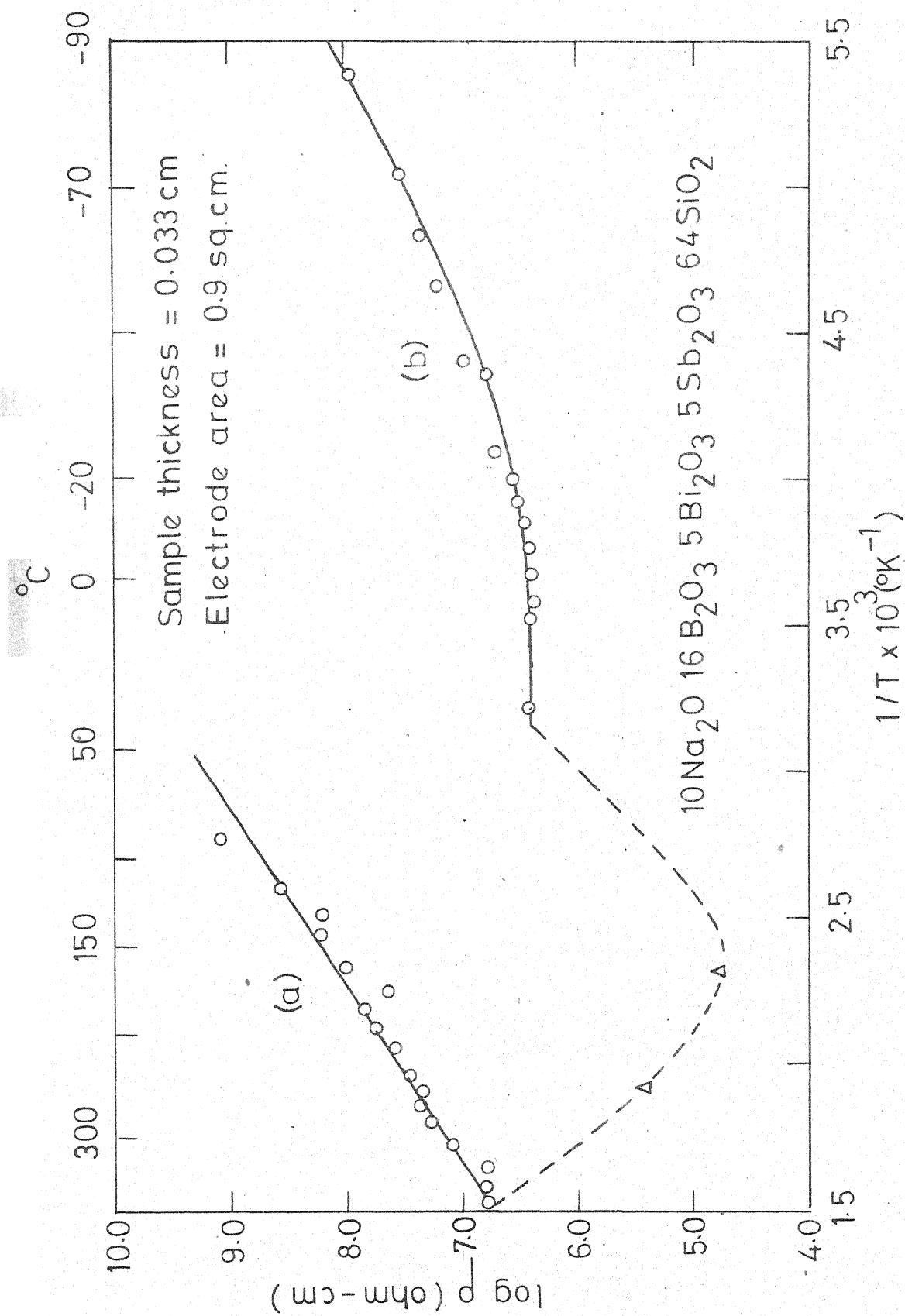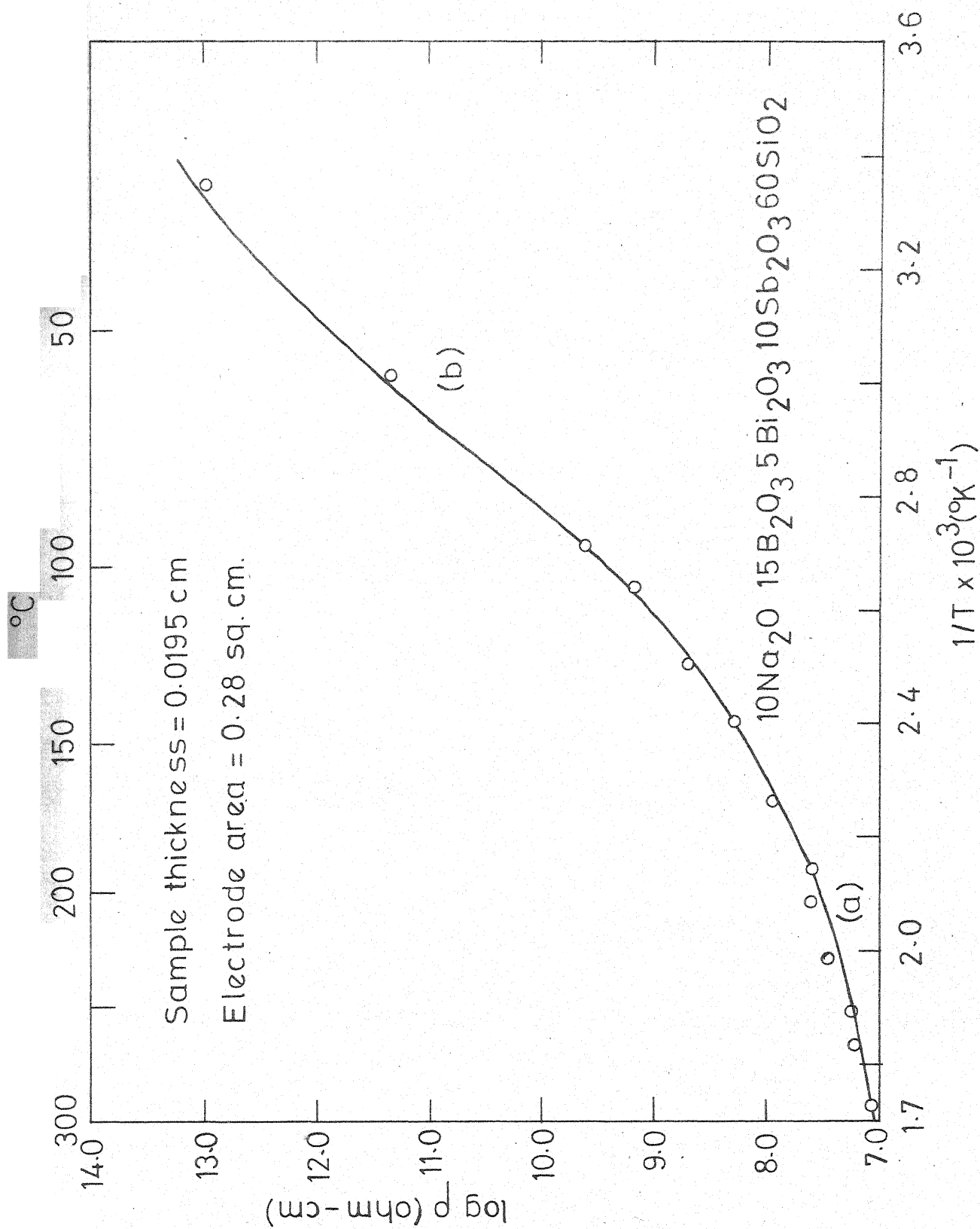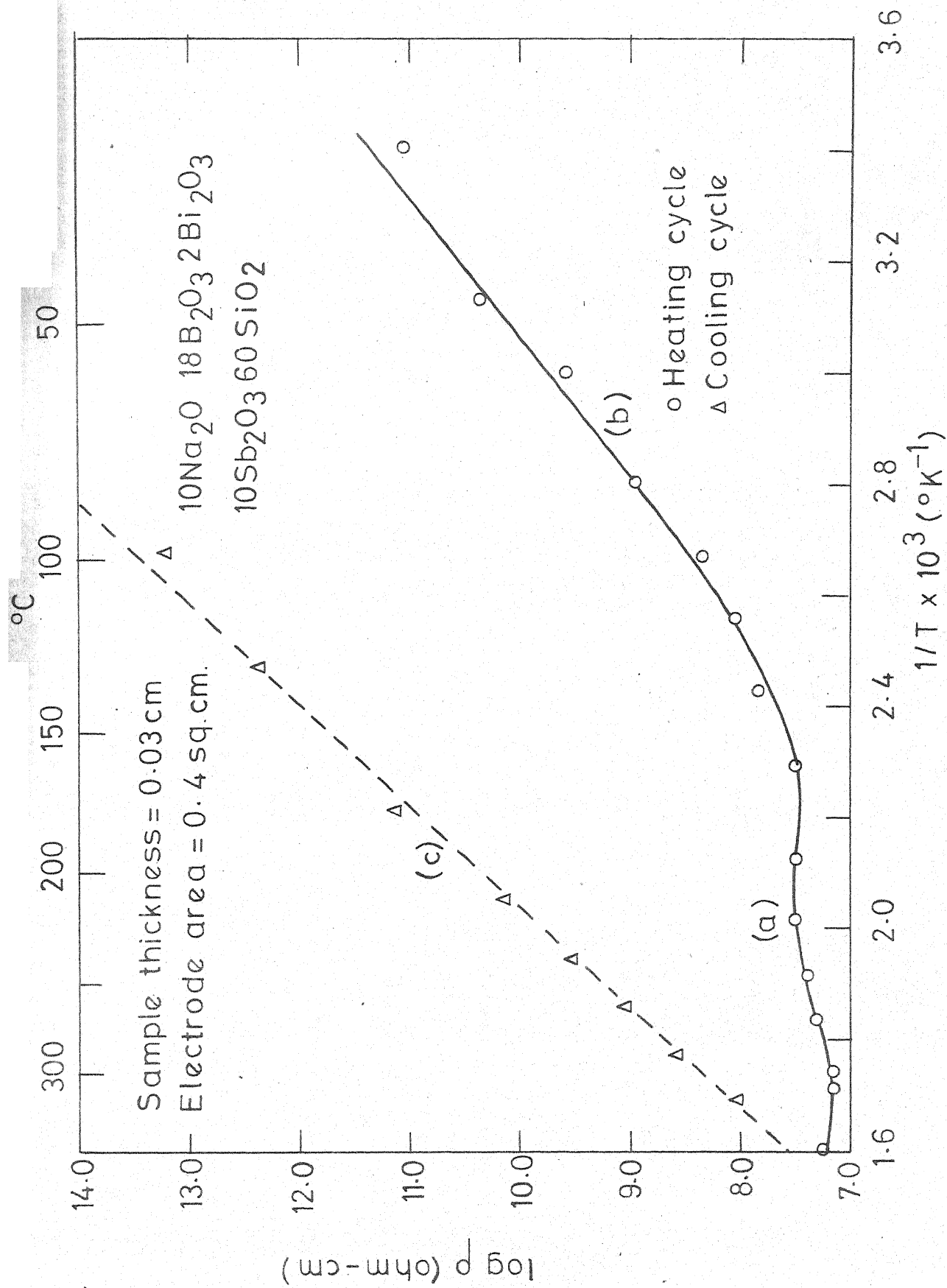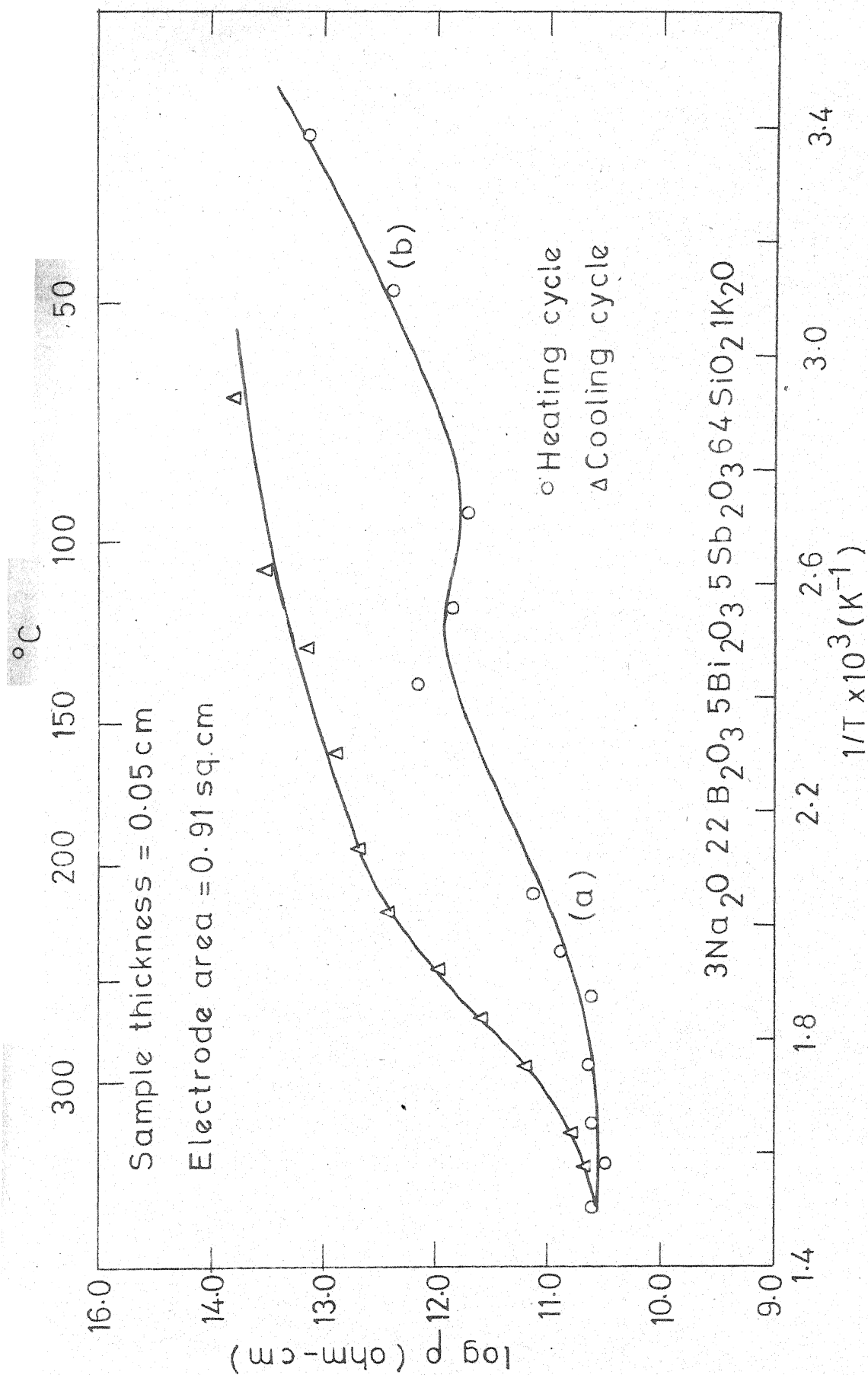
Fig. 4 Variation of bulk resistivity with temperature for glass 3.

Fig. 5 Variation of bulk resistivity with temperature for glass 4.

Fig. 5 Variation of bulk resistivity with temperature for glass 5.

Fig. 7 Variation of bulk resistivity with temperature for glass 12.
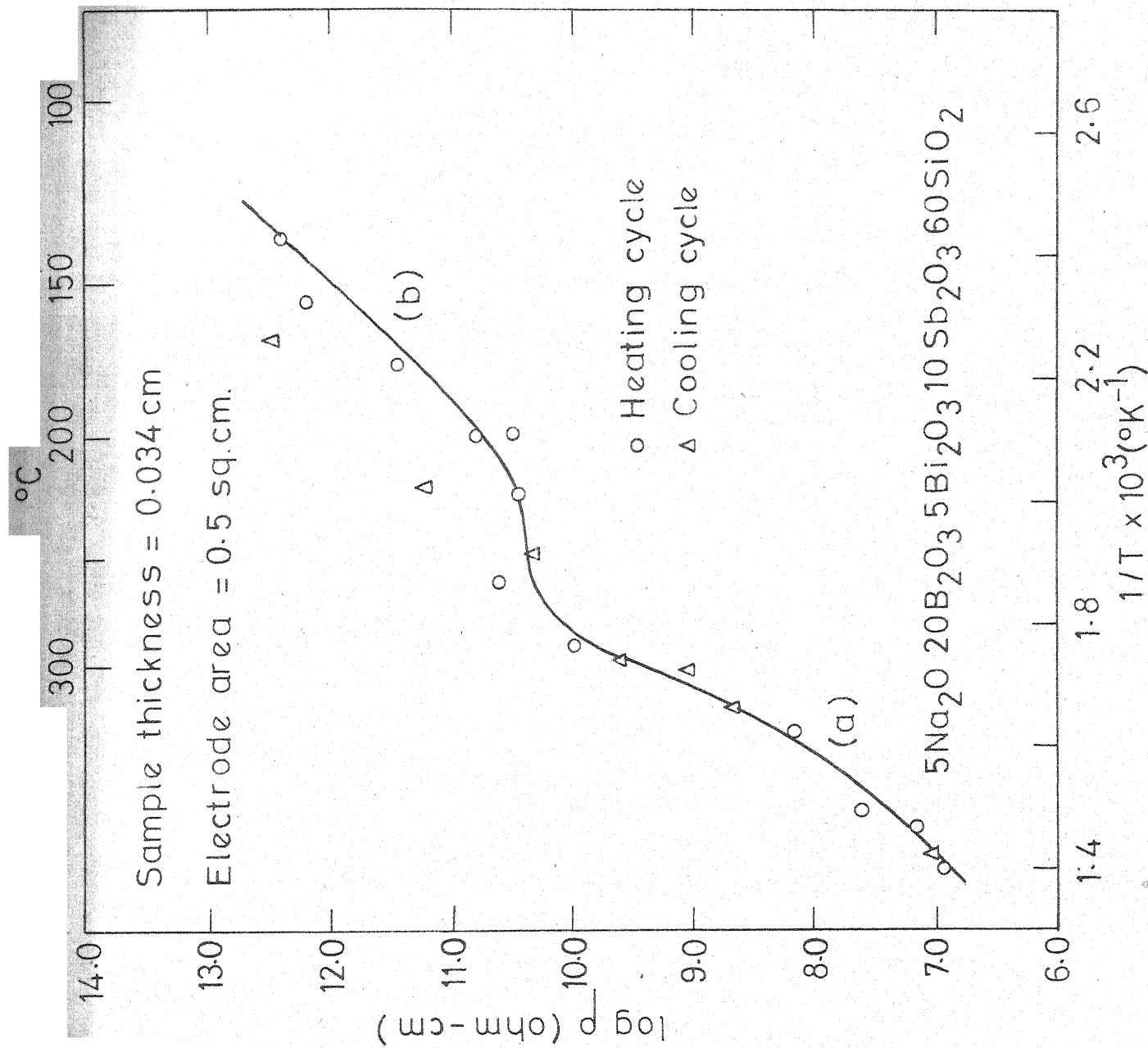
°C

Sample thickness = 0.034 cm

Electrode area = 0.5 sq.cm.

o Heating cycle
Δ Cooling cycle

(b)

(a)

$5Na_2O\ 20B_2O_3\ 5Bi_2O_3\ 10Sb_2O_3\ 60SiO_2$

log ρ (ohm-cm)

$1/T \times 10^3 (°K^{-1})$

Fig. 8 Variation of bulk resistivity with temperature for
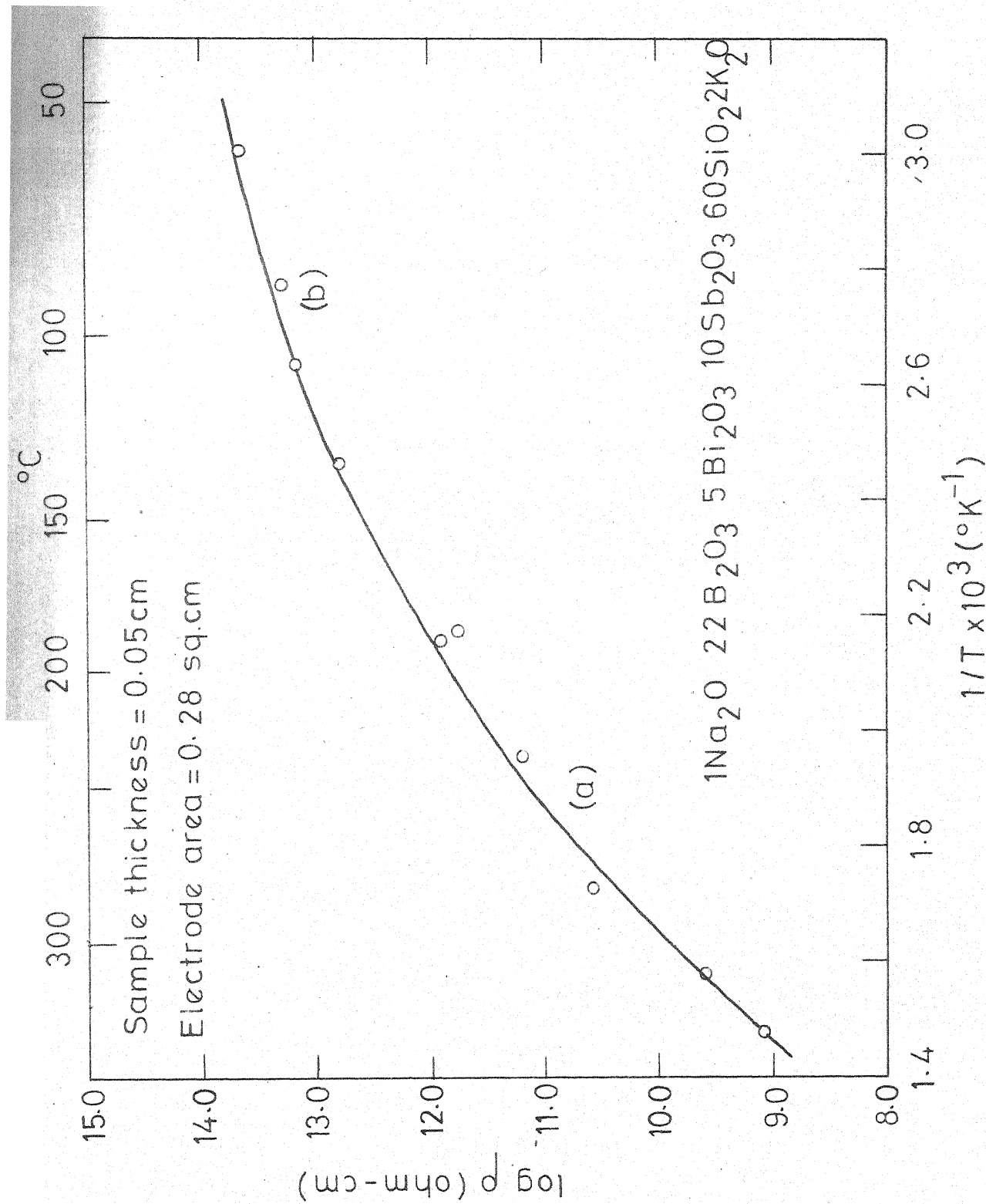
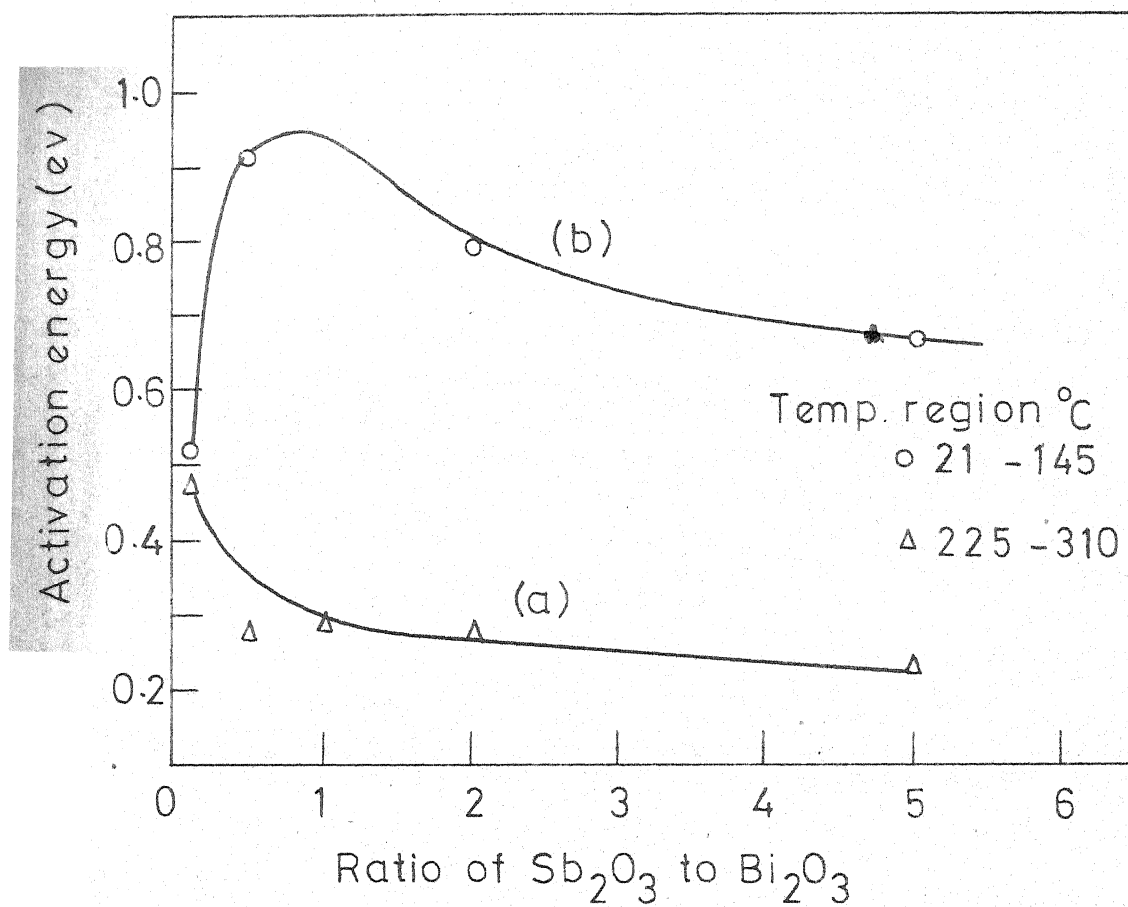Fig. 9 Variation of bulk resistivity with temperature for glass 23.

Fig. 10 Variation of activation energy with ratio of concentration of Sb_2O_3 to Bi_2O_3.
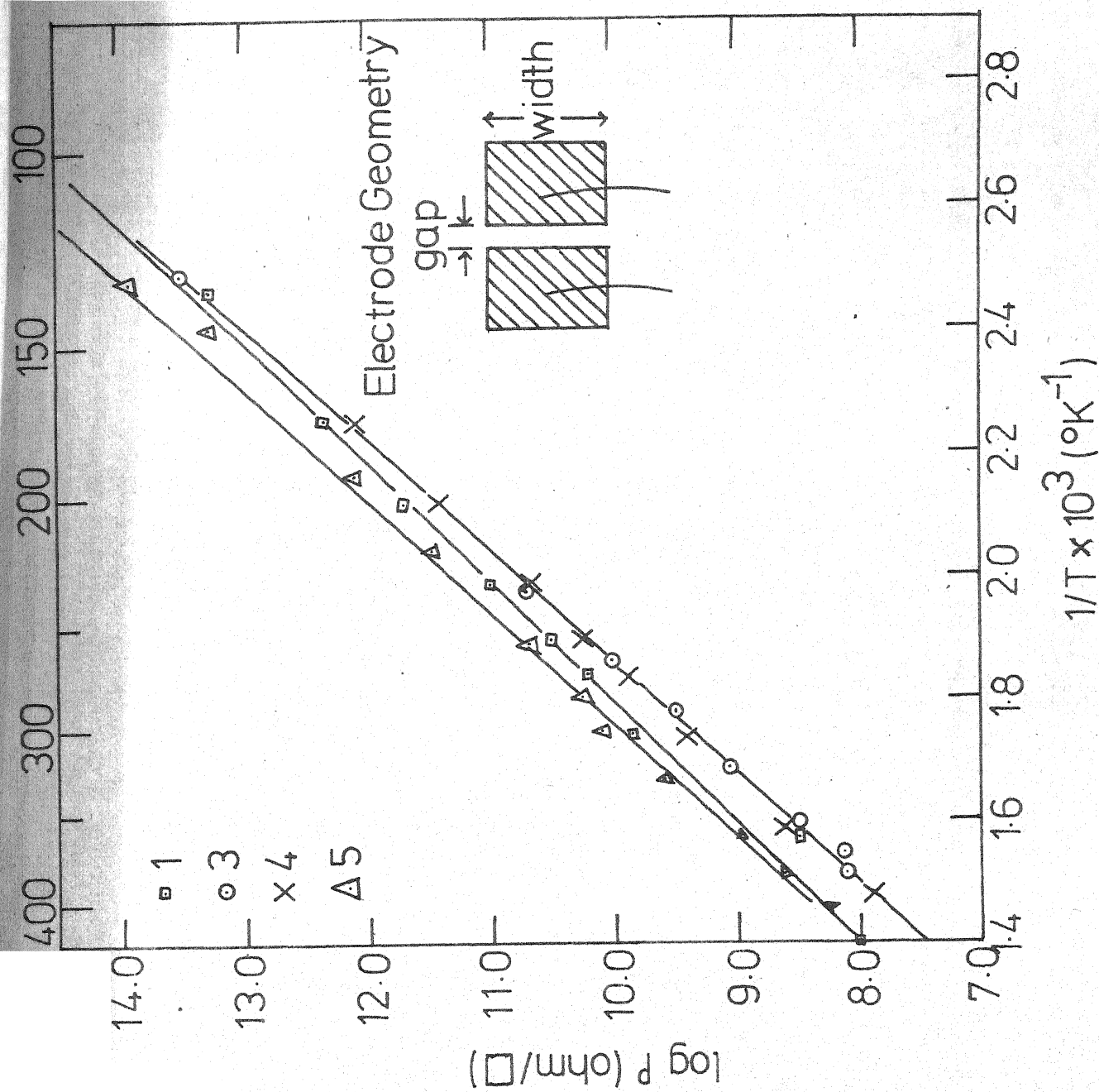
Fig.11 VARIATION OF SURFACE RESISTIVITY OF VIRGIN
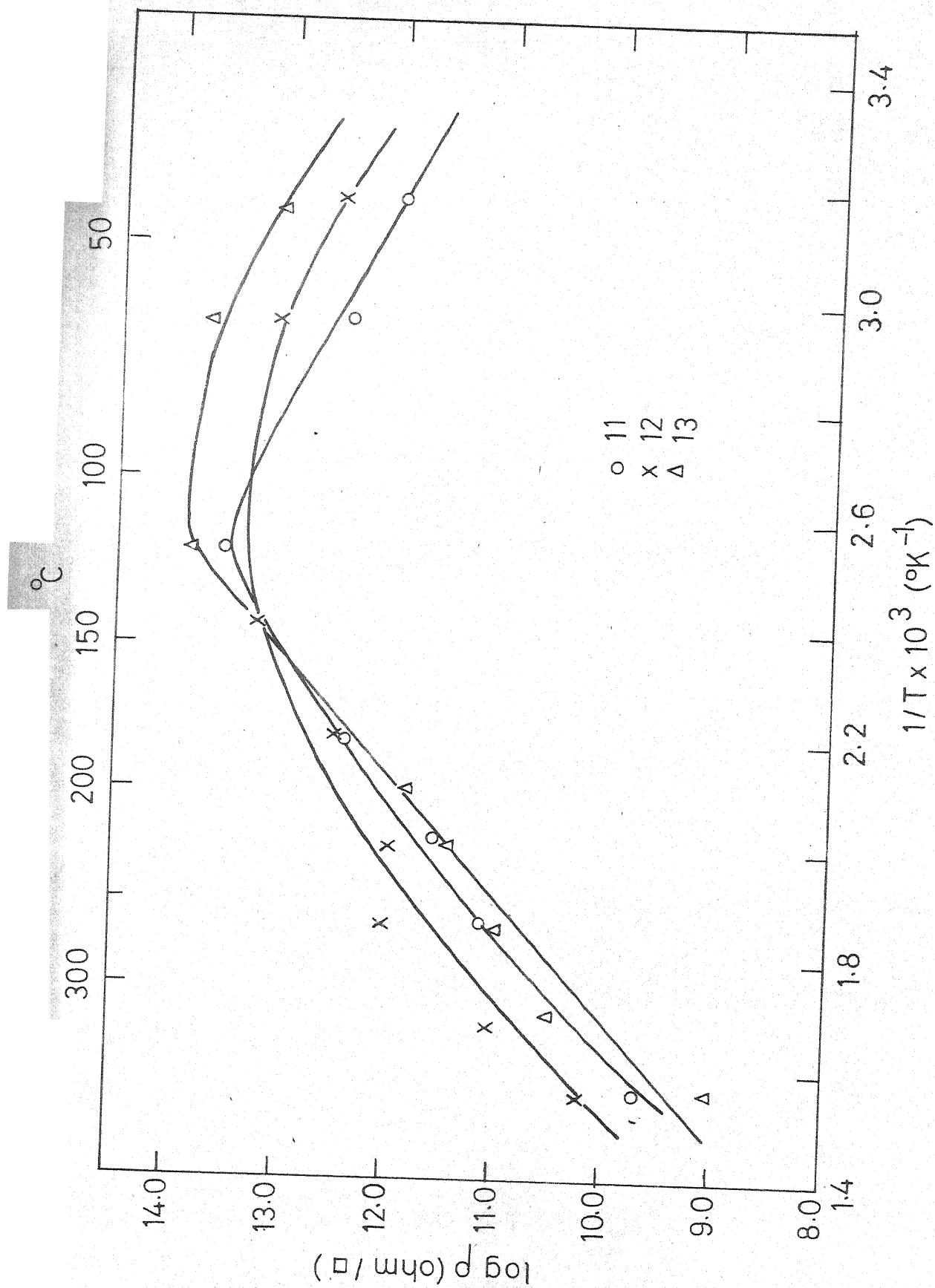GLASSES WITH TEMPERATURE

Fig. 12 Variation of surface resistivities of virgin glasses 11, 12 and 13 with temperature

°C

Glass no.   2   3
Electrode
width   1·2 cm   1·4 cm
Electrode
gap   0·065cm 0·115cm

           Na₂O B₂O₃ Bi₂O Sb₂O₃ SiO₂

No.2   10   15   10   5   60
   3   10   16   5   5   64

o Heating cycle
△ Cooling cycle

3

(b)

1

(a)

(b)

2

log ρ (ohm / □)

12·0
11·0
10·0
9·0
8·0
7·0

300   200   150

50

1·6   2·0   2·4   2·8   3·2
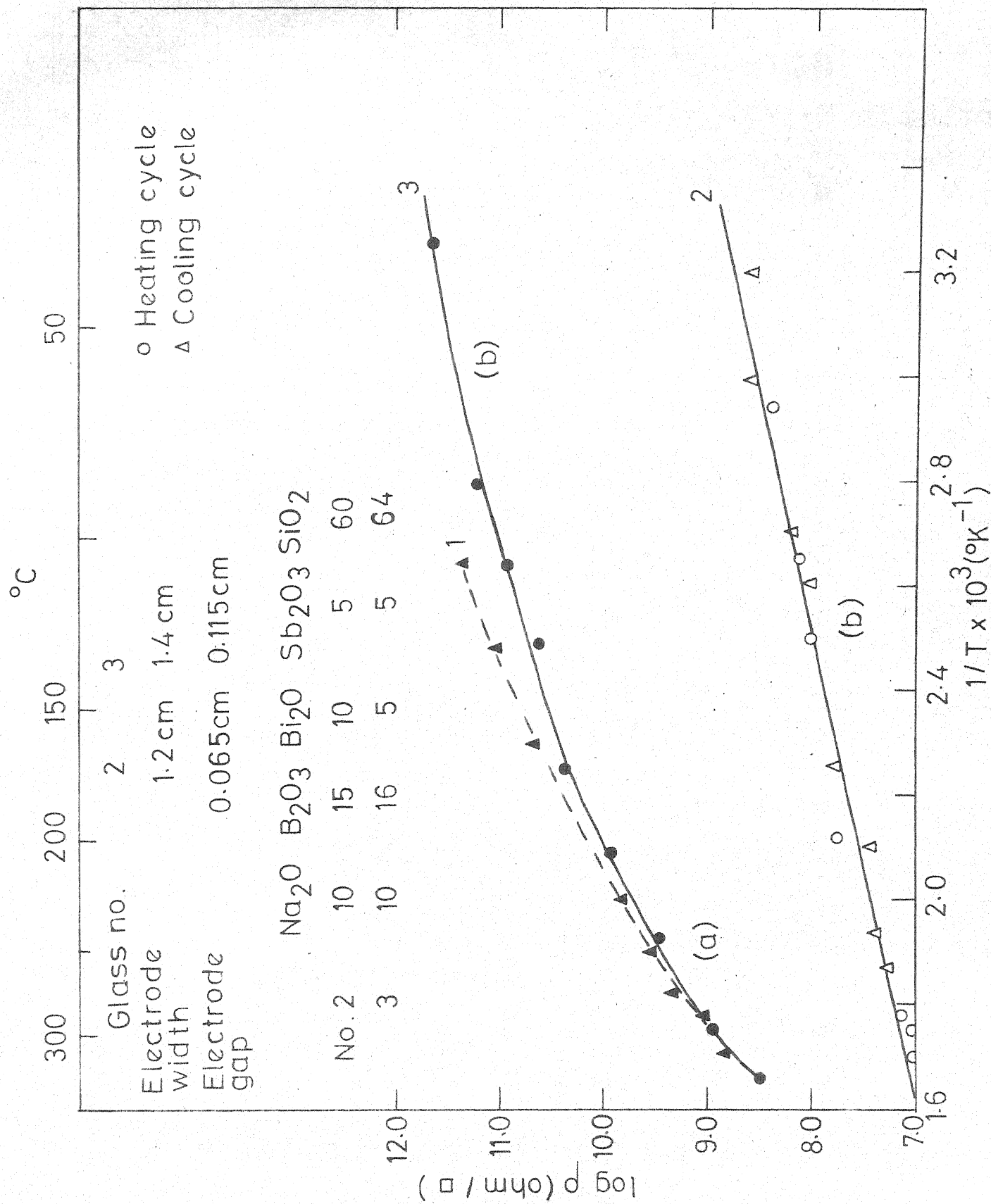
1/T x 10³(°K⁻¹)

FIG. 13 Variation of surface resistivities of reduced glass 2 & 3 with temperature
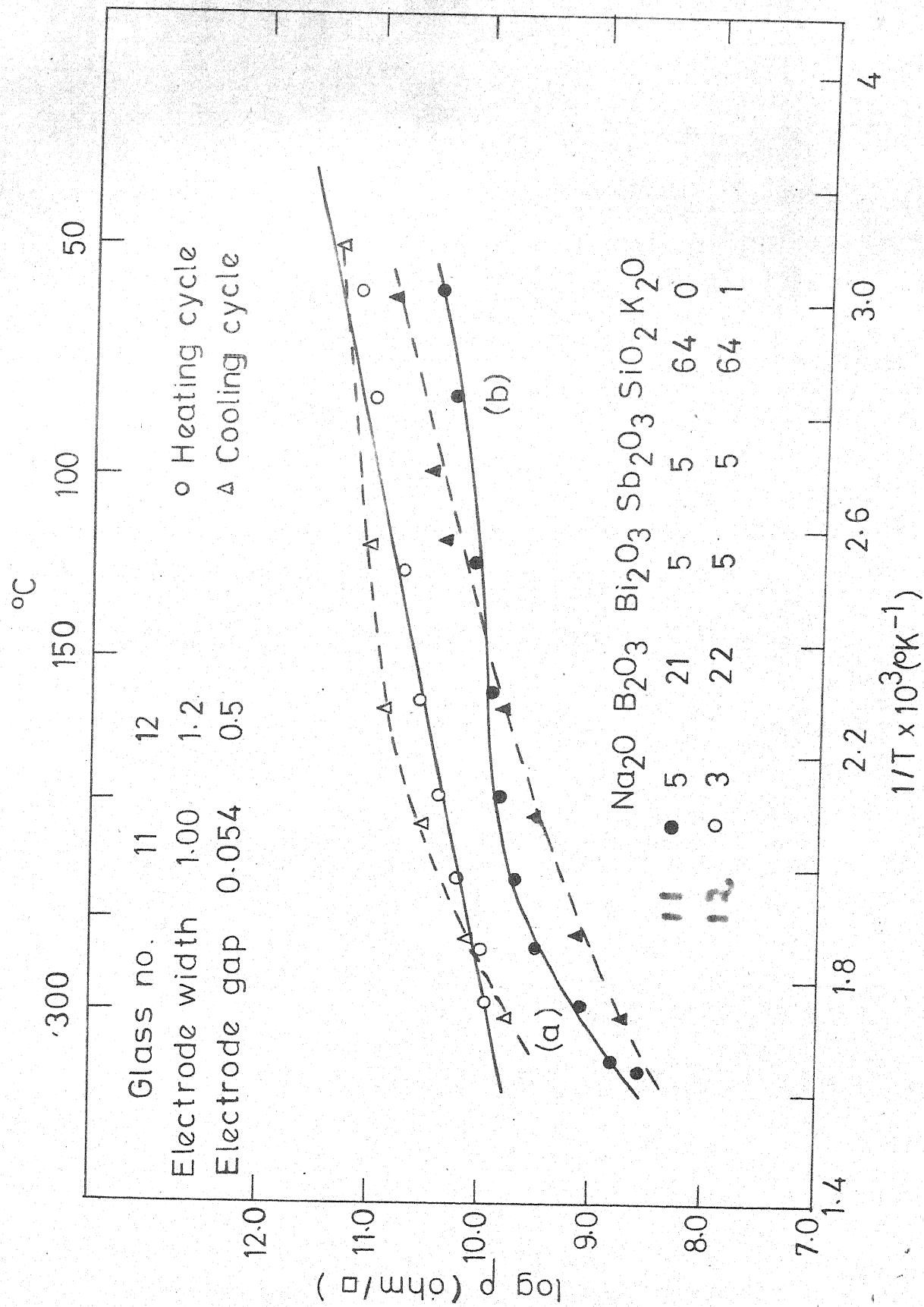
Fig. 14 Variation of surface resistivity of reduced glasses 11 & 12 with temperature
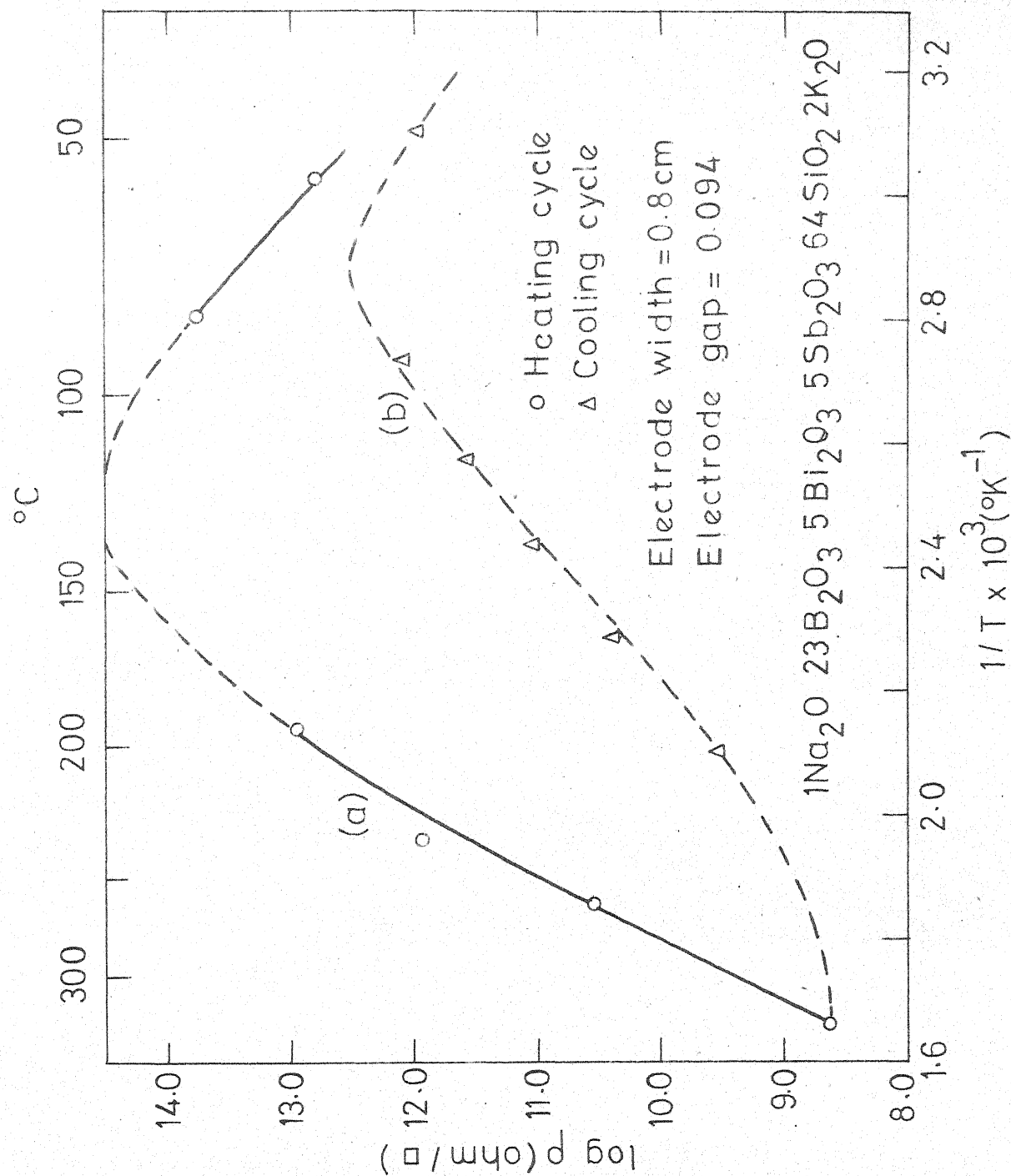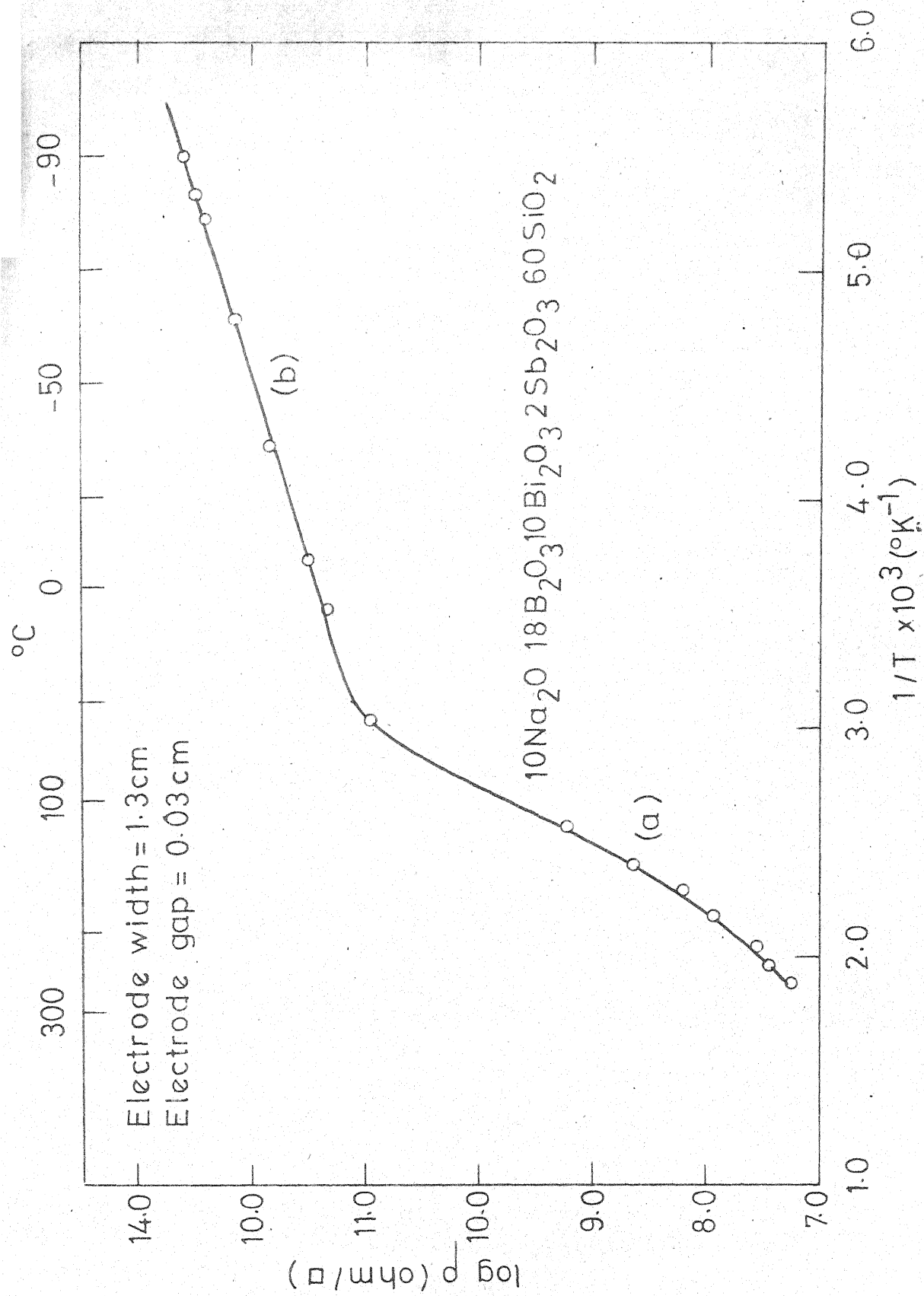
Fig. 15 Variation of surface resistivity of reduced glass 13 with temperature

Fig. 16 Variation of surface resistivity of ion-exchanged and reduced glass 1

Fig. 17 Variation of surface resistivity of IER glass 2 with temperature

Fig. 18 Variation of surface resistivity of IER glass 3 with temperature

The figure shows a plot with axes:
- y-axis: log ρ (ohm/□), ranging from 7.0 to 14.0
- x-axis (bottom): 1/T × 10³ (°K⁻¹), ranging from 1.8 to 3.4
- x-axis (top): °C, with markings at 250, 150, 100, 50

Labels on plot: (a), (b)

Electrode width = 1.3 cm.
Electrode gap = 0.15 cm.
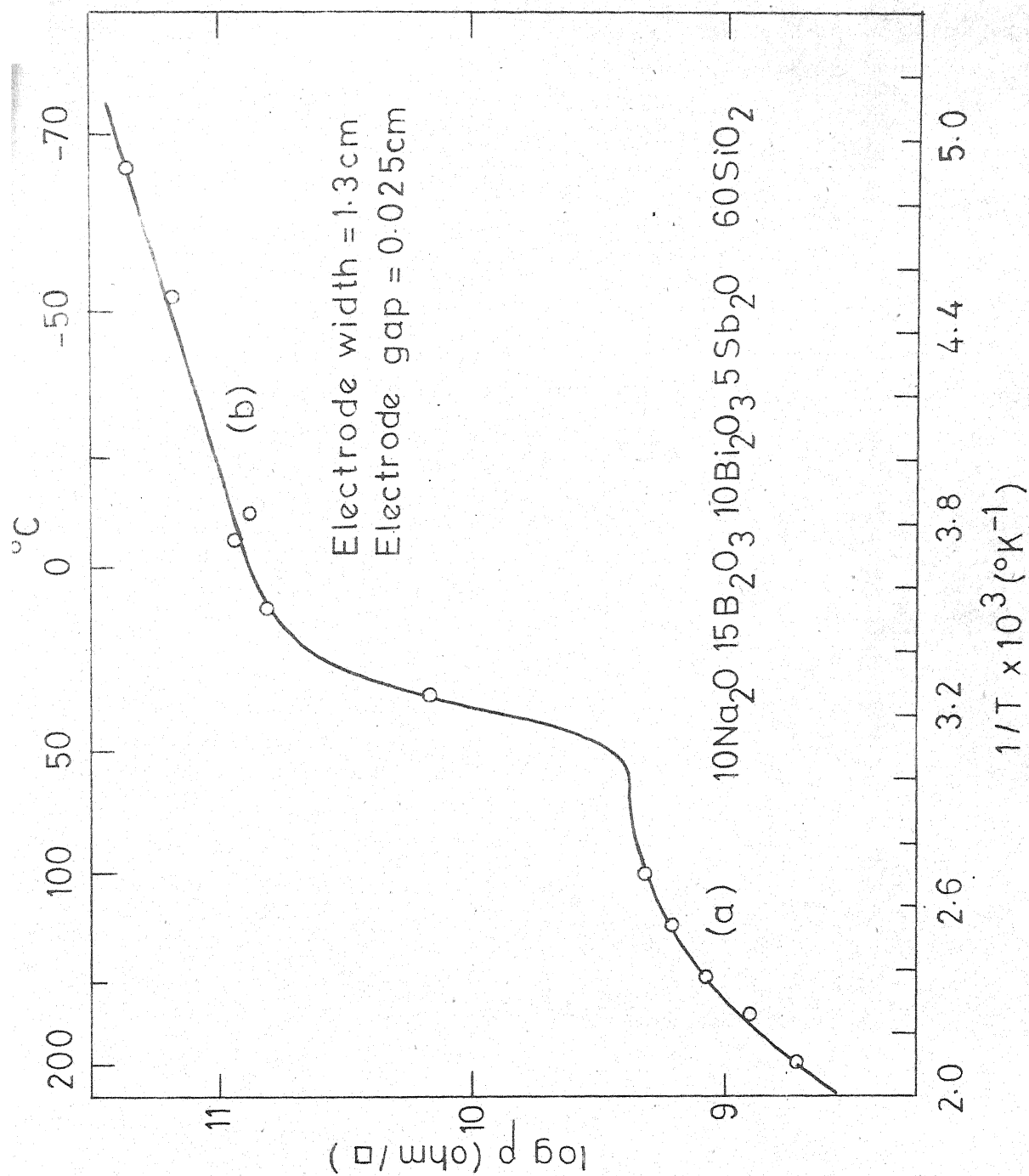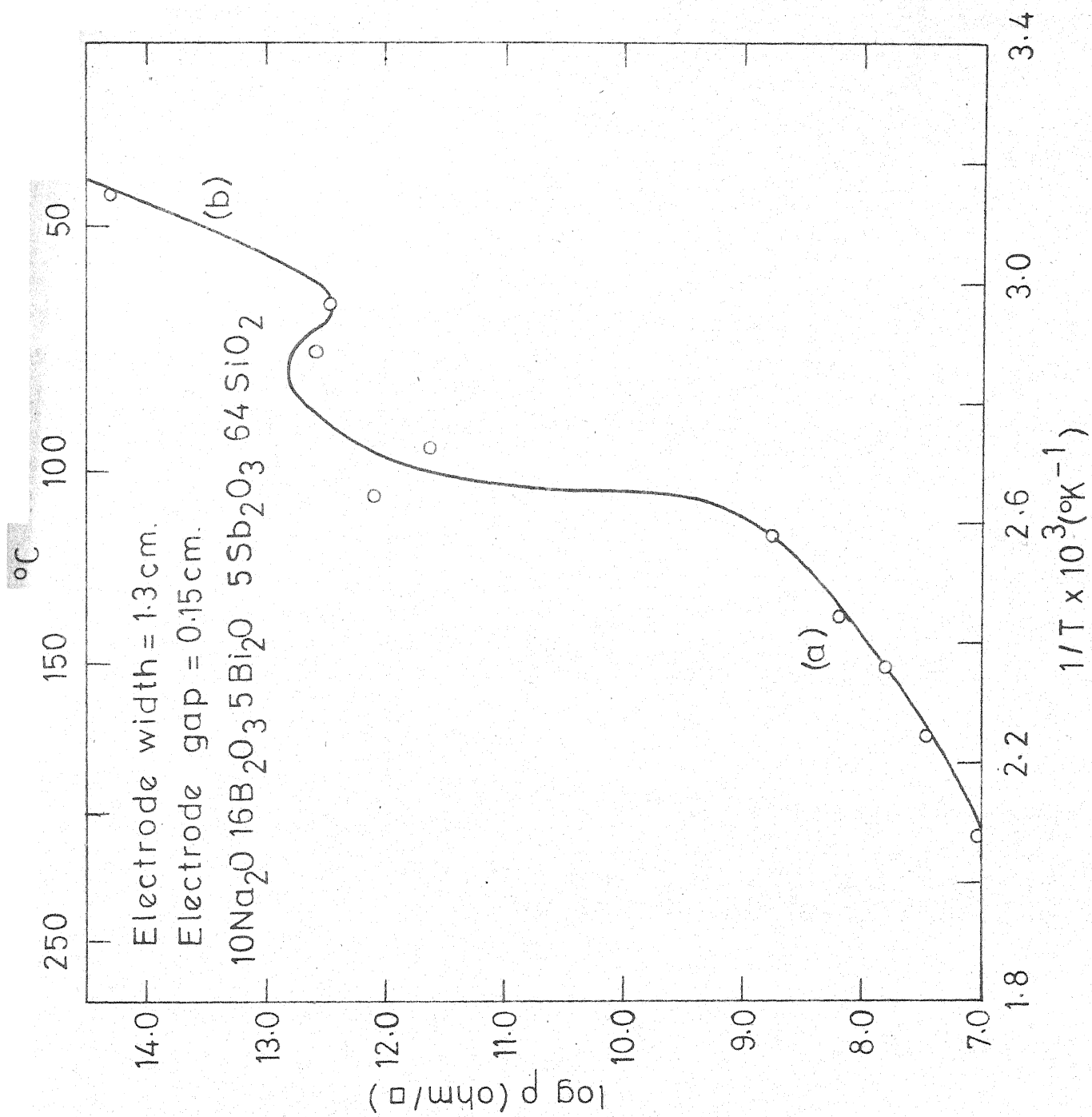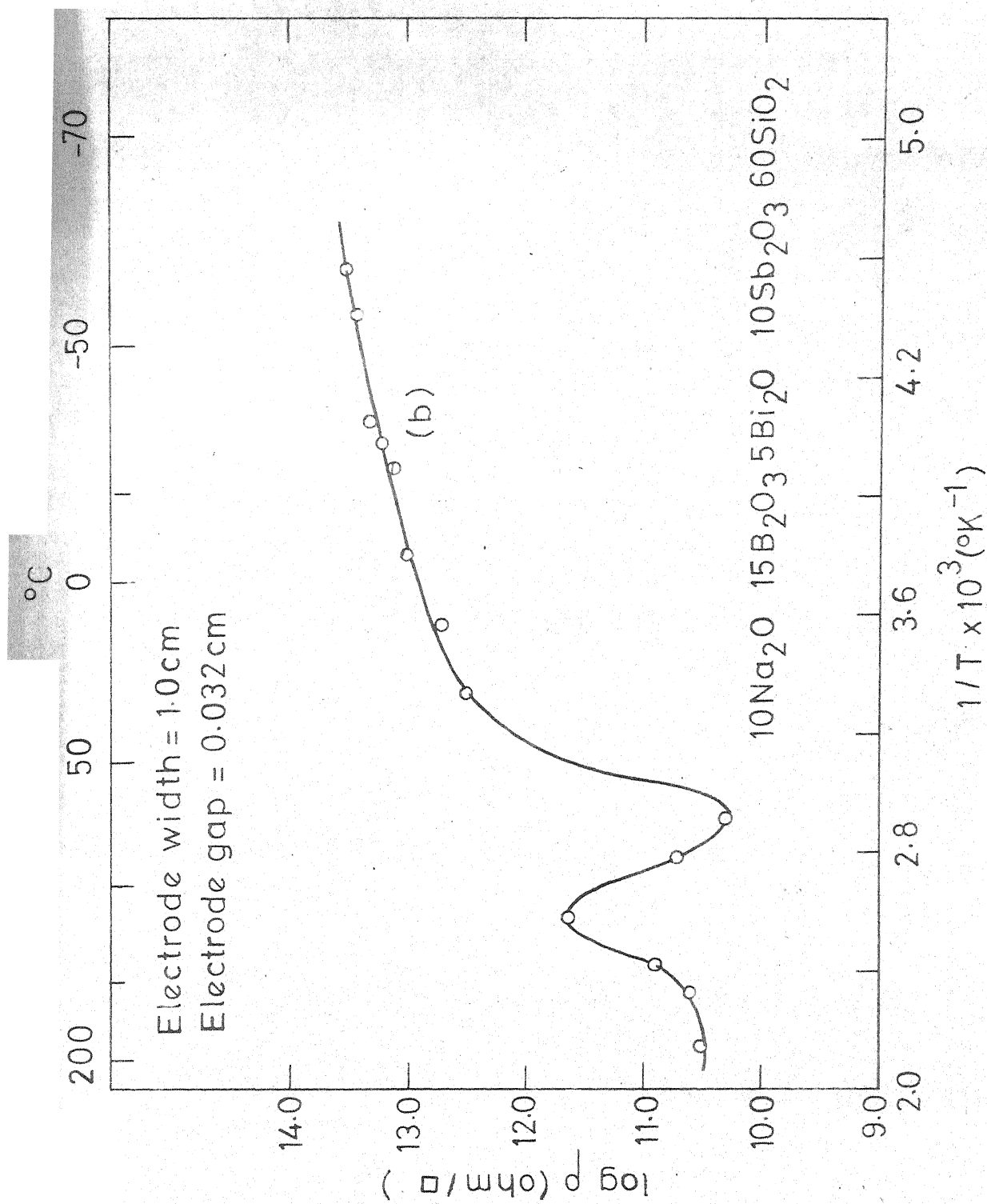10Na₂O 16B₂O₃ 5Bi₂O 5Sb₂O₃ 64SiO₂

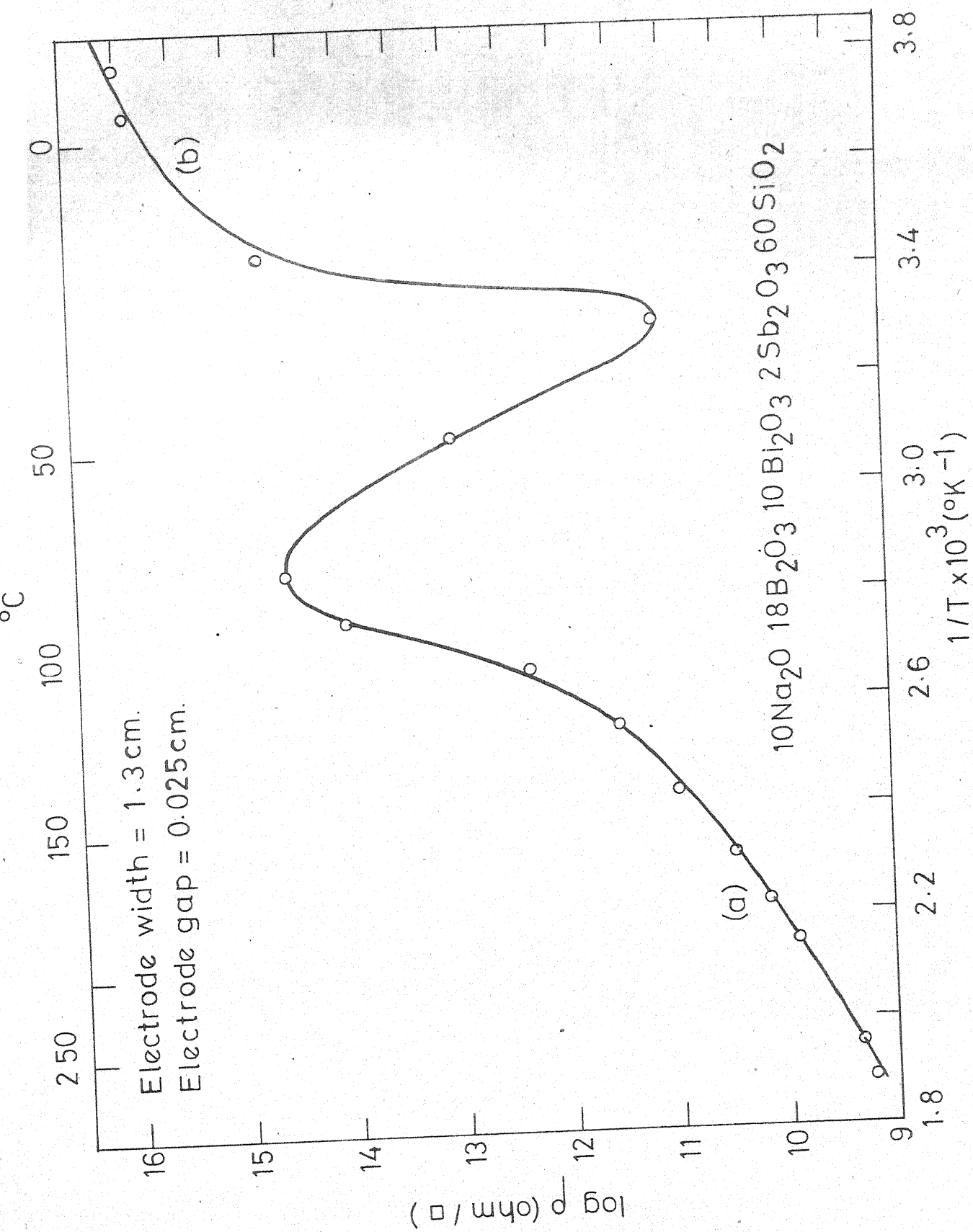Fig. 19 Variation of surface resistivity of IER glass 4 with temperature

Fig. 20 Variation of surface resistivity of IER glasses 5 with temperature

Fig. 21 Variation of surface resistivities of IER glass 11 with temperature

Fig. 22 Variation of surface resistivity of IER glass 12, 13 & 22 with temperature

Fig. 23 Variation of surface resistivity of IER glass 21 with temperature

Within the figure:

Electrode width = 0.8 cm
Electrode gap = 0.076 cm

o Heating cycle
△ Cooling cycle

$5\ Na_2O\ 20\ B_2O_3\ 5\ Bi_2O_3\ 10\ Sb_2O_3\ 60\ SiO_2$

y-axis: log ρ (ohm / □), 7.0, 8.0, 9.0, 10.0, 11.0, 12.0, 13.0

x-axis (top): °C, 50, 100, 150, 200, 300

x-axis (bottom): $1/T \times 10^3 (°K^{-1})$, 1.6, 2.0, 2.4, 2.8, 3.2

Fig. 24   Switching characteristics of IER glasses 1, 2 & 4

Fig. 25 Plot of $\sqrt{\alpha h\nu}$ vs. $h\nu$ for different glasses (Numbers in bracket indicate thickness of specimen in mm)

Fig. 26 DTA curves for virgin glasses 2 and 3

CHAPTER V

DISCUSSION

5.1 Bulk Resistivity

For bulk resistivity, the log ρ vs 1/T plots show
two distinct activation energies. The variation of resis-
tivity with temperature and activation energy values which
are about 1 eV, for the glasses indicate that the conductivity
would arise due to movement of alkali ions. For glasses
1, 2, 4, 5 and 12 there is deviation from linearity at high
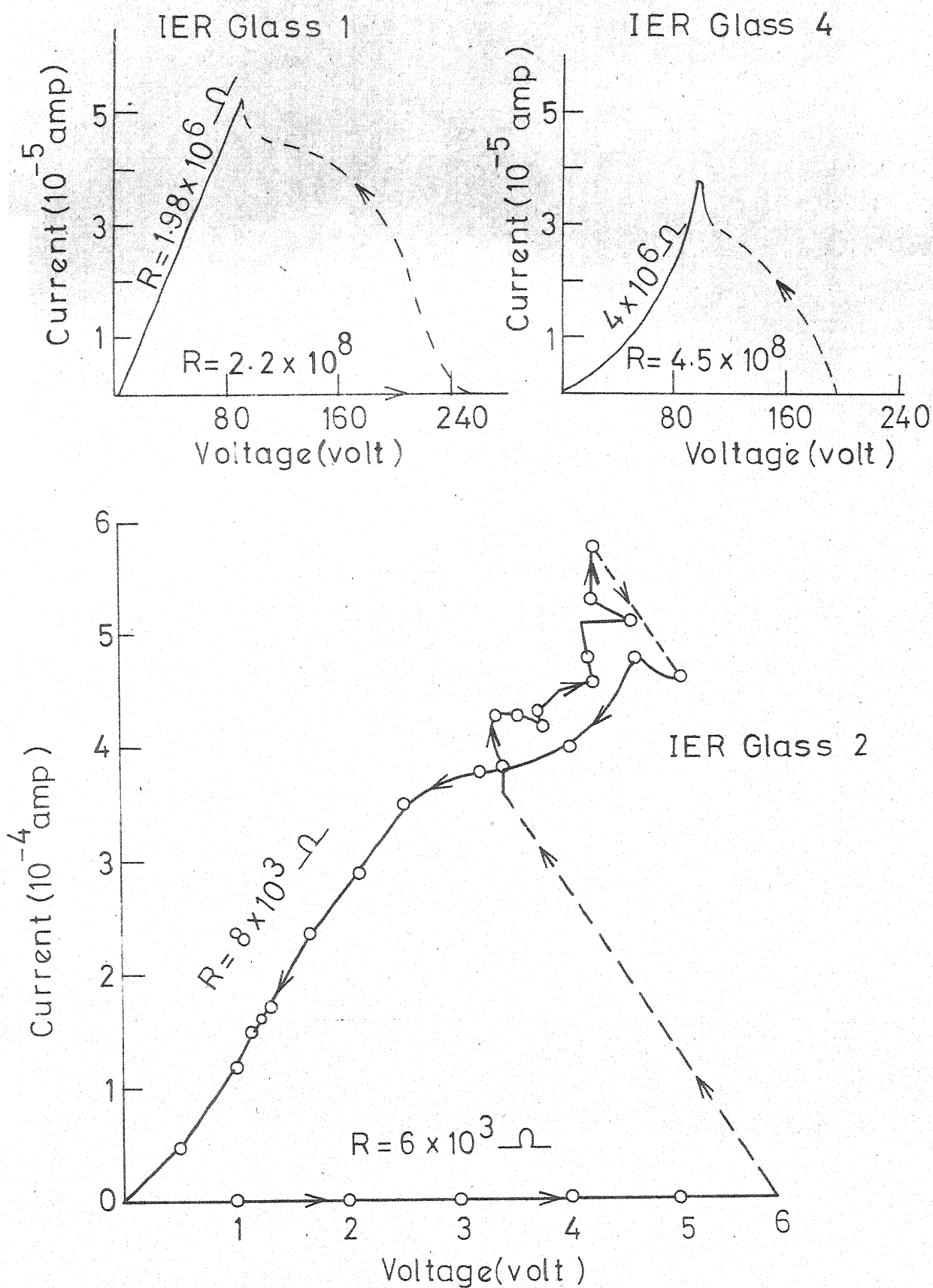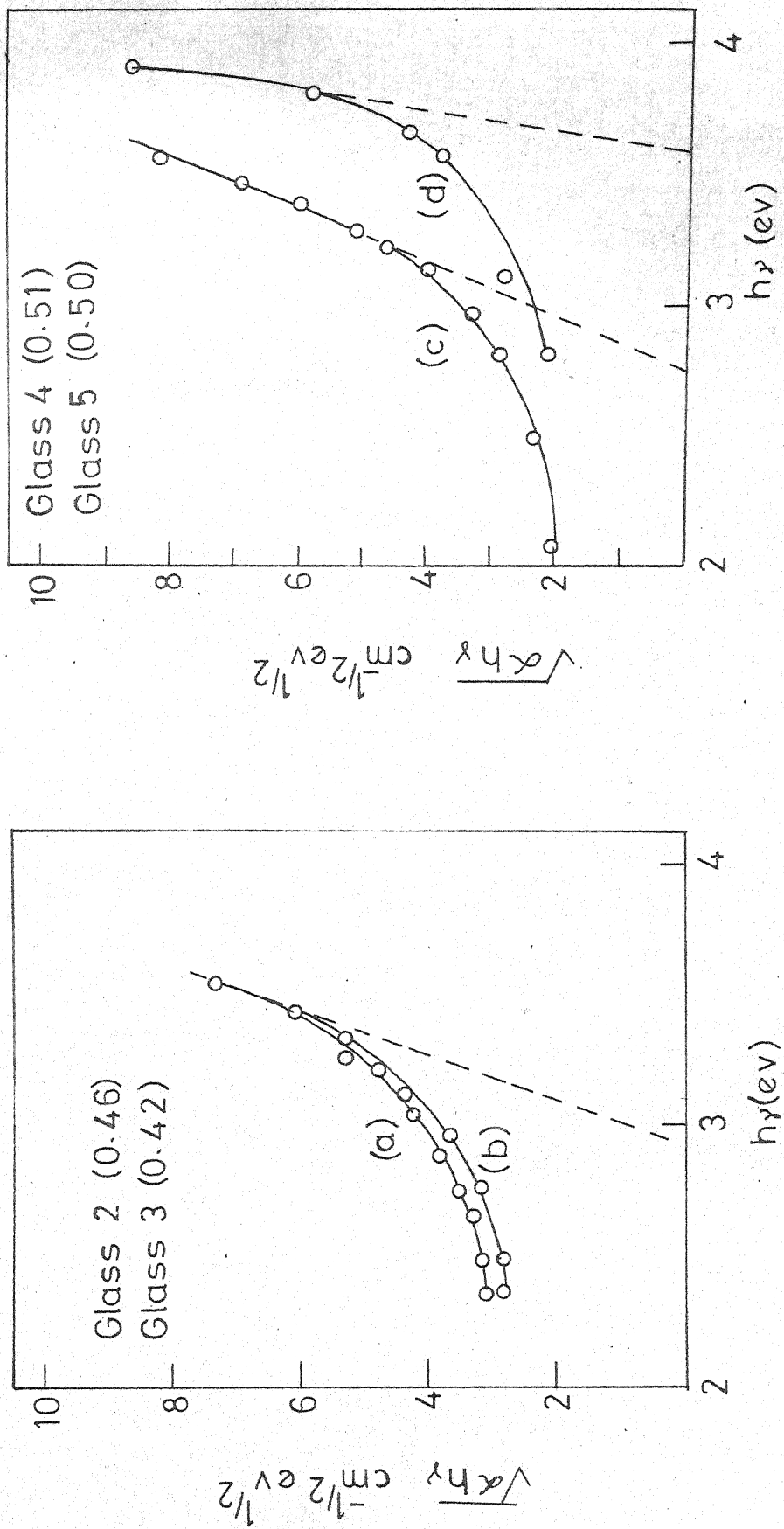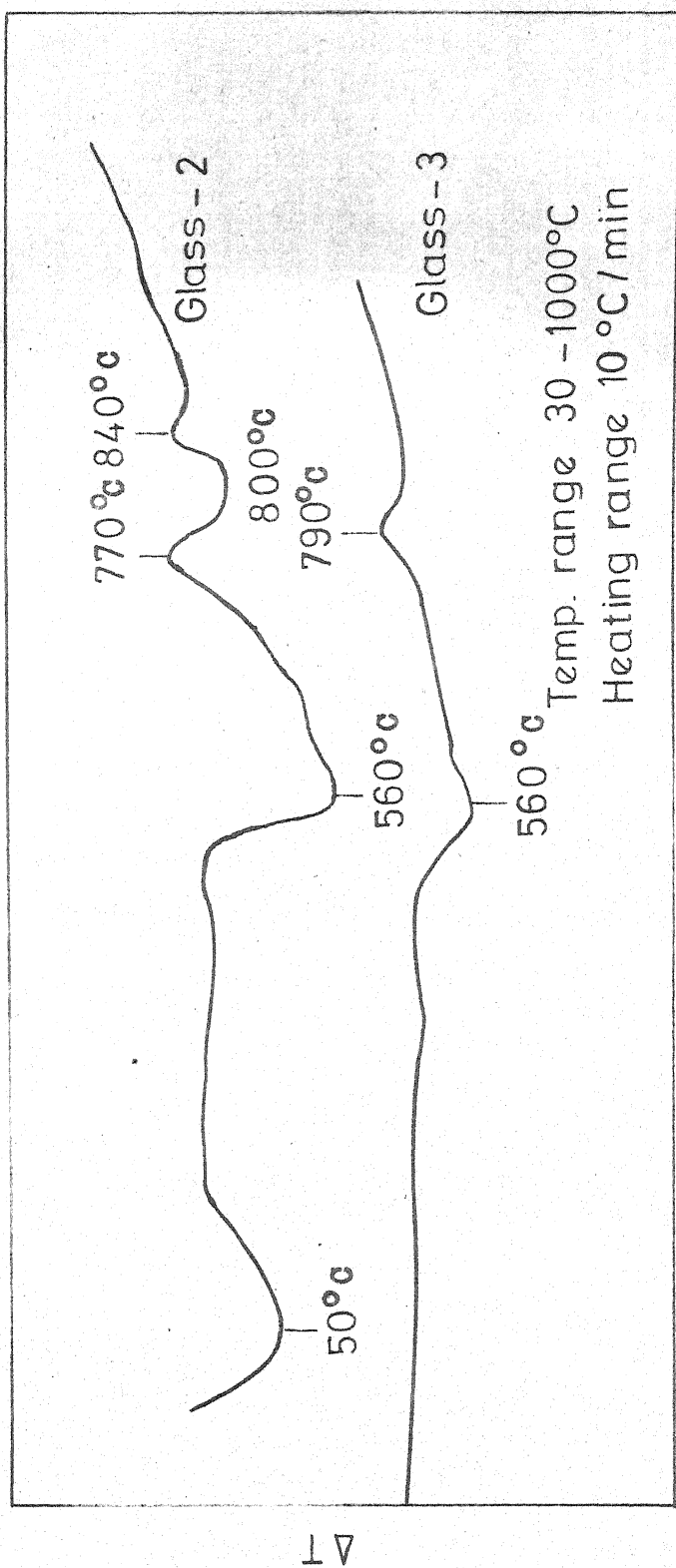temperatures. This could be due to polarisation at the
electrodes. The charges collect at the electrodes and
resist the flow of charge carriers which is responsible for
high resistance. The fact that glass 23 which contains less
mole % of Na_2O does not show polarisation may support the
fact the conduction in these glasses is due to sodium ions.
However, it is to be noted that for all the glasses the
linearity of I-V plots was maintained. This casts some
doubt on the above explanation of polarisation effect. In
order to confirm the effect of polarisation, one should
carry out a.c. measurements for these glasses.

In Fig. 10, the variation of activation energy
with the ratio of concentration of Sb_2O_3 to Bi_2O_3 is

shown. We observe a peak in activation energy when the ratio Sb_2O_3/Bi_2O_3 is about one. This may be explained as follows. In the borosilicate glasses containing both Sb_2O_3 and Bi_2O_3, bismuth can be considered to act as network modifier, and antimony can be considered to act both as network former as well as network modifier.[67] It may be possible that as the ratio of Sb_2O_3/Bi_2O_3 increases first Sb^{3+} ions occupy the "network forming" sites and the network becomes more and more rigid. The activation energy would thus increase. When the ratio Sb_2O_3/Bi_2O_3 becomes unity, Sb^{3+} ions may start acting as network modifier like Bi^{3+} ions. The network becomes less and less rigid, lowering the activation energy.

For the temperature range 225 to 310°C in the plot of activation energy vs. the ratio of Sb_2O_3/Bi_2O_3 (Fig. 11) there is no peak in the activation energy. At the high temperature Sb^{3+} ions may not act as network former but may act as network modifier, which accounts for lowering of the activation energy as Sb_2O_3/Bi_2O_3 increases. The activation energy is lower at high temperature which is characteristic of ionic conduction. However, this explanation might have to be reviewed seriously if electrode polarization effect is proved to be dominant in this temperature range.

In some of the glasses cooling curves show linear behaviour and differ from heating curves. This could be attributed to the effect of heat treatment given to the sample during heating cycle.

5.2 Surface Resistivity

Borosilicate glasses containing As_2O_3 and Sb_2O_3 have shown peculiar behaviour in the variation of surface resistivity with temperature[59,63]. It has been observed that in these glasses, as the temperature is increased from room temperature the resistivity increases (which is contradictory to usual behaviour) upto certain temperature and then it decreases. Whereas, when the temperature is decreased from room temperature, there was a sudden increase of resistivity. Thus the resistivity has a dip at the room temperature. This has been explained as follows.

It has been assumed that, water molecules adsorbed on the surface do play a role in determining the surface resistivity. The increase of resistivity with temperature has been explained due to protons acting as charge carriers. Protons are thought to be present in hydroxyl group and these migrate to near by terminal oxygen atoms under the action of an electrical field[65]. Conductivity increases

with the concentration of both the OH groups and the terminal oxygen atoms. Since the sum of these concentrations is constant, there is an optimum ratio of concentration at which conductivity is greatest.

As the temperature of sample is increased from room temperature, some of water molecules may be driven off and hence the surface resistivity is increased. Above a certain temperature, the decrease in surface resistivity has been explained as of alkali ions. As the temperature is lowered below room temperature the sudden increase of resistivity has been explained due to the upsetting of the optimum ratio between the concentration of OH groups and terminal atoms, as the water content is increased.

Since our glasses under investigation have similar glass matrix as in the case of As_2O_3 or Sb_2O_3, one would expect the similar behaviour for our glass also. We shall discuss this in detail in next sections.

5.2.1 <u>Virgin glasses</u>

For glasses 1, 3, 4 and 5 (with 10 mole % Na_2O) the plots of log ρ vs. 1/T are as shown in figure 11. The plots are all linear and the activation energies are of the order of 1 eV. Glasses 11, 12 and 13 (with 5, 3, 1 mole % Na_2O respectively) show a peak in the resistivity

The orders of the magnitudes of surface resistivities of the reduced glasses 2, 3, 11 and 12 (Figs. 13 and 14) are much less than that of the virgin glasses (Figs. 11 and 12). This may be attributed due to presence of conducting islands of bismuth and antimony as shown from microstructural studies. The activation energies for reduced glasses are of the order 0.3 eV compared to 1 eV for virgin glasses. One possibility for lowering of the activation energy is that it arises from electron hopping between two conducting islands, as the conduction mechanism in the reduced glasses.

For glass 13 (Fig. 15), the order of magnitude of surface resistivity is comparable to that of virgin glasses. This can be explained as for the glass 13 reduction may not be complete. Perhaps, low concentration of Na_2O may cause partial reduction.

5.3.3 Ion-exchanged and reduced glasses

5.3.3.1 Low temperature measurements

In the low temperature regions of the plots log ρ vs. 1/T, for IER glasses (figures 17 to 20) we see that the activation energies are low as given in Table 2. The low activation energy observed in low temperature

region for the glasses can be attributed to electron
hopping between conducting islands as explained below.

As discussed in Chapter I, the microstructure of
ion-exchanged and reduced glasses containing Bi_2O_3 and
Sb_2O_3 separately has been shown to consist of a dispersion
of particles of antimony, bismuth and silver. These are
considered to act like conducting islands. The diameter of
these conducting islands of bismuth can be approximately
calculated using Neugebauer and Webb model[64]. The
activation energy ($\emptyset$) as given by the model is

$$\emptyset = \frac{e^2}{Kr}$$

where e = charge of electron; K = dielectric constant of
glass matrix, and r = size of conducting islands. Assum-
ing a value of K = 6 and $\emptyset$ = 0.08 eV for our glass system,
we get r = 45 Å. This is consistent with the microstructural
features of the glasses.

5.2.3.2 High temperature measurements

The plots of log ρ vs. 1/T for ion-exchanged and
reduced glasses show peculiar behaviour. By comparing
the plots of log ρ vs. 1/T for IER glasses and virgin
glasses we find in the temperature range

about 50-520°C. The orders of magnitudes of surface
resistivities of FBR glasses are less than that of the
virgin glasses. As in the case of reduced glasses, this
can also be attributed to the presence of conducting
islands.

We observe peaks and dips in the plots for glass
2, 3, 4, 5 and 21 as shown in figures (17-20 and 23. By
comparing the plots we see that as the ratio of concentration of Sb_2O_3 to Bi_2O_3 decreases

(i)   The peaks and dips disappear gradually (there is no
      peak for glass 1 where the ratio Sb_2O_3/Bi_2O_3 is 0.2
      as shown in Fig. 16).

(ii) Temperature at which the minimum resistivity occurs,
      shifts towards higher temperature (for glasses 5, 4,
      3, 2 and 21 the temperature shifts from room temper-
      ature to 70°C).

In borosilicate glasses containing As_2O_3 and
Sb_2O_3 separately, similar peculiarities with temperature
have been observed. But for those glasses minima of
resistivity have been found to occur always at room temper-
ature. This behaviour has been explained as the effect
of adsorption of water by the glass surfaces as described
earlier.

about 50-320°C. The orders of magnitudes of surface resistivities of IER glasses are less than that of the virgin glasses. As in the case of reduced glasses, this can also be attributed to the presence of conducting islands.

We observe peaks and dips in the plots for glass 2, 3, 4, 5 and 21 as shown in figures 17-20 and 23. By comparing the plots we see that as the ratio of concentration of Sb_2O_3 to Bi_2O_3 decreases

(i)   The peaks and dips disappear gradually (there is no peak for glass 1 where the ratio Sb_2O_3/Bi_2O_3 is 0.2 as shown in Fig. 16).

(ii) Temperature at which the minimum resistivity occurs, shifts towards higher temperature (for glasses 5, 4, 3, 2 and 21 the temperature shifts from room temperature to 70°C).

In borosilicate glasses containing As_2O_3 and Sb_2O_3 separately, similar peculiarities with temperature have been observed. But for those glasses minima of resistivity have been found to occur always at room temperature. This behaviour has been explained as the effect of adsorption of water by the glass surfaces as described earlier.

However, the above explanation may not hold good in explaining the nature of variation of log ρ with $1/T$ for glasses containing both Sb_2O_3 and Bi_2O_3 since the temperature at which the minimum of resistivity occurs, shifts towards the high temperature. Perhaps, the water adsorption may not play a role in conduction process for our glass systems.

As we know there will be drastic changes in the physical properties of materials undergoing structural transitions. One can also expect that some sort of structural transition may be occurring in our glass systems. The dips and peaks of the plots of log ρ vs. $1/T$ may then be considered to arise from some structural transition which may be taking place in these glasses at the particular temperature.

However, the above observed nature of the variation of resistivity with temperature for our glass systems may be due to the combined effect of antimony, bismuth and silver particles as these are shown to be present in ion-exchanged and reduced glasses.

In order to confirm whether the behaviour is due to water adsorption or not one should carry out the measurements in vacuum or by passing dry nitrogen over the sample.

5.3 Switching

IER glasses 1, 2 and 4 have been found to show
"memory type" switching. As explained in Chapter 1, the
switching in the IER glasses containing Bi_2O_3 could probably
arise due to a crystallisation process induced in the glass
phase between the metallic particles. The same process
may also be thought of to be effective in the glasses under
investigation. Further studies have to be done on glasses
containing both Sb_2O_3 and Bi_2O_3 in order to find the combined
effect of these oxides.

5.4 Optical Absorption

For virgin glasses 2, 3, 4 and 5, the absorption
edge was observed at about 3000 Å. The absorption edges
lie in the range of 2.7 to 3.7 eV. As we see, these are
more than twice the activation energy determined by d.c.
measurements for these glasses. This is consistent with
the results of other oxide glasses[23].

5.5 Differential Thermal Analysis

DTA curves for glasses 2 and 3 show an endothermic
peak at about 560°C and exothermic peak at about 790°C.
The endothermic peak may be thought of as arising due to

crystallisation. However when heat treatment was given to glass 2, no crystallisation was observed. This would cast doubt on the above explanation. An endothermic peak at about 50°C for glass 2 may be due to expelling of water molecules adsorbed in the glasses.

CHAPTER 6

CONCLUSION AND SCOPE FOR FURTHER WORK

6.1 Conclusions

From the experimental studies, made on the borosodasilicate glasses containing both Sb_2O_3 and Bi_2O_3, the following conclusions could be drawn.

(i) The rigidity of borosodasilicate glass matrix depends on the ratio of concentration of Sb_2O_3 to Bi_2O_3 and the network coherence seems to be maximum when the ratio is one.

(ii) The d.c. electrical conductivity of these glasses in the temperature range 50-400°C is due to the motion of alkali ions.

(iii) The orders of magnitudes of surface resistivities of the reduced and the ion-exchanged and reduced glasses are less than that of virgin glasses and this is attributed to the presence of conducting islands of either antimony or bismuth or silver or a combination of these three.

(iv) The surface resistivities of ion-exchanged and reduced glasses show dips and peaks in the plots of log ρ vs. 1/T. The minima of the surface

resistivity move toward high temperature as the ratio of the concentration of Sb_2O_3 to Bi_2O_3 decreases. This behaviour cannot be attributed to the effect of water adsorption and may be considered to arise from some structural transitions occurring in these glasses at these temperatures.

(v) Conduction in the ion-exchanged and reduced glasses at low temperatures arises due to the electron hopping between the conducting islands. This is consistent with the microstructural features of the glasses.

6.2 Scope for Further Studies

(i) To study in detail the microstructure of the glasses and to characterise the different phases before and after the surface treatments (like ion-exchange or reduction) given to them.

(ii) The variations of surface resistivities of the glasses containing Bi_2O_3-Sb_2O_3, As_2O_3 and Sb_2O_3 with temperature have showed peculiar behaviour. It will be interesting to study the variation of surface resistivities of borosoda glasses containing combinations of above ingredients like As_2O_3-Bi_2O_3, Sb_2O_3-As_2O_3.

(iii) In order to study the effect of water adsorption of the glasses, it is necessary to carry out the measurements in vacuum or in an inert atmosphere.

REFERENCES

1. R.G. Neale, J. Non-cryst. Solid, 2 (1970) 558.

2. D. Pai and S.W. Ing, Phy. Rev., 173 (1968) 729.

3. E.P. Denton, H. Rawson and J.E. Stanworth, Nature, London, 173 (1954) 10.

4. J.D. Mackenzie, "Semiconducting Oxide Glasses" in Modern Aspects of the Vitreous State, ed. J.D. Mackenzie, Vol. 3 (1964), Butterworths (Washington).

5. J.D. Mackenzie, J. Am. Ceram. Soc., 47 (1964) 211.

6. R. Tsu et.al., J. Non-cryst. Solids, 4 (1970) 322.

7. A.M. Andreiesh and B.T. Kolomiets, Soviet Phys. Solid State, 6 (1965) 2652.

8. M.H. Bodsky et.al., Phys. Rev. B1, (1970) 2632.

9. H.L. Uphoff and J.H. Healy, J. Appl. Phys., 32 (1961) 950.

10. J.T. Edmond, J. Non-cryst. Solids, 1 (1958) 39.

11. H. Fritsche, 'Electronic & Structural Properties of Amorphous Semiconductors.

12. R. Callerbs, M. Denayer, F.H. Hashmi and G.D. Petit, Discussions of Faraday Soc., 50 (1970) 27.

13. L. Banyai, Physique des semiconductors (Dunod, Paris, 1960) 147.

14. N.F. Mott, Advan. Phys., 16 (1967) 49.

15. E.A. Fagen and H. Fritzsche, J. Non-cryst. Solids, 2 (1970) 170, 180.

16. M. Pollak & T.H. Geballe, Phy. Rev., 122 (1961) 1742; M. Pollak, Phys. Rev., 133 (1964) A564.

17. A.E. Owen and J.M. Robertson, J. Non-cryst. Solids, 2 (1970) 40.

18 H.P.D. Lanyon, Phys. Rev., 130 (1961) 134.

19. J.L. Hartke, Phys. Rev., 125 (1962) 1177.

20. B.T. Kolomietes and E.A. Lebdev, Soviet Phy. Semiconductors, 1 (1967) 244.

21. R.S. Allgaier, in: Proc. 9th Intern. Conf. on the Physics of Semiconductors, Moscow,(1968).

22. M.D. Tabak and P.J. Warter, Phys. Rev., 173 (1968) 729.

23. Y. Toyozawa, Tech. Report of the Inst. for Solid State Physics (Univ. of Tokyo) Ser. A No. 119 (1964).

24. H.P.D. Lanyon, Phys. Rev., 125 (1962) 1177.

25. J. Tauc,in: Optical Properties of Solids, Ed. F. Abeles (North Holland, Amsterdam, 1969).

26 T.M. Donovan, and W.E. Spicer, Phys. Rev. Letters, 21 (1968) 1572.

27. J.T. Littleton and G.W. Morey, The Electrical Properties of Glass, Wiley, New York, 1953.

28. E. Rasch and F. Hinrichsen, Z. Electrochem., 14 (1908) 41.

29. J. Frenkel, Kinetic Theory of Liquids, Oxford Univ. Press, London, (1946).

30. J.M. Stevels, Encyclopedia of Physics, Vol. 20, 350, Springer-Verlag, Berlin (1957).

31. O.V. Mazurin, Electrical Properties and Structures of Glass, Consultants Bureau, New York (1965).

32. R.H. Doremus, in: Modern Aspects of the Vitreous State, Vol. 2, Chap. 1, Butterworths, Washington D.C. (1962).

33. R.H. Doremus, J. Phys. Chem., 68 (1964) 2212.

34. B. Lengyel and Z. Boksay, Z. Phys. Chem., 203 (1954) 93; 204 (1955) 157.

35. J.O. Isard, J. Non-cryst. Solids, 1 (1969) 235.

36. J.R. Johnson, R.H. Bristow and H.H. Blau, J. Am. Ceram. Soc., 34 (1965) 135.

37. R.J. Charles, J. Am. Ceram. Soc., 45 (1962) 105.

38. J.T. Littleton and W.L. Wetmore, J. Amer. Ceram. Soc., 10 (1936) 243.

39. M.H. Cohen, H. Fritzsche and S.R. Ovshinsky, Phys. Rev. Letters, 22 (1969) 1065.

40. N.F. Mott, Advan. Phys., 16 (1967) 49.

41. N.F. Mott, Phil. Mag., 22 (1970) 7.

42. N.F. Mott and E.A. Davis, Electronic Processes in Non-crystalline Materials, Clarendon Press, Oxford, 1971.

43. P.W. Anderson, Phys. Rev., 109 (1958) 1492.

44. A.1. Gubanov, Quantum Theory of Amorphous Conductors, Consultants Bureau, New York, 1965.

45. K. Hulls and P.W. Mcmillan, J. Phys. D. Appl. Phy., 5 (1972) 67.

46. A.D. Pearson, J. Non-cryst. Solids, 2 (1970) 1.

47. H.R. Fritzsche, J. Non-cryst. Solids, 2 (1970) 393.

48. K.W. Boer and S R. Ovshinsky, J. Appl. Phys., 41 (1970) 2675.

49. A.D. Pearson, IBM J. Res. Develop., 13 (1969) 510.

50. S.R. Ovshinsky, J. Non-cryst. Solids, 2 (1970) 99.

51. J.J. O'Dwyer, J. Electrochem. Soc., 116 (1969) 239.

52. D. Eaton, J. Am. Ceram. Soc., 47 (1964) 554.

53. **R.L. Green and K.B. Blodsett, J. Am. Ceram. Soc.,** 31 (1948) 89.

54. K.B. Blodgett, J. Am. Ceram. Soc., 34 (1951) 14.

55. A.K. Varshneya, J. Non-cryst. Solids, 19 (1975) 355.

56. D. Chakravorty, J. Non-cryst. Solids, 15 (1974) 191.

57. D. Chakravorty, A. Shuttleworth and P.H. Gaskell, J. Materials Science, 10 (1975) 799.

58. D. Chakravorty, Appl. Phys. Letters, 24 (1974) 62.

59. Devendra Kumar . M.Tech. Thesis, I.I.T. Kanpur (1975).

60. D. Chakravorty and C.S. Murthy, J. Phys. D. Appl. Phys., 8 (1975) 2162.

61. D. Chakravorty, to be published.

62 W.H. Omar, M. El. Hamamsy and A. Bishay, Proc. 9th Int.
    Congr. on Glass, Versailles (1971) 521.

63. Halliyal Arvind, M.Tech. Thesis, I.I.T. Kanpur (1976).

64. C.A. Neugebauer and M.B. Webb, J. Appl. Phys., 33
    (1962) 74.

65. S. Iizima, M. Surgi, M. Kikuchi and K. Tanaka, Solid
    State Communications, 9 (1971) 795.

66. J. Tauc et.al., in Physics of Non-crystalline Solids,
    Ed. J.A. Prins, North Holland, Amsterdam (1965) 606.

67. J. Stanworth, Physical Properties of Glasses, Oxford,
    Clarendon Press (1953).